MONITORING OF DAMAGE IN PRESTRESSING TENDONS USING ULTRASONIC GUIDED WAVES

A thesis report submitted in the partial fulfillment of the
requirement for the award of degree of

MASTER OF ENGINEERING
IN
STRUCTURES

Submitted By:

Naveen Sachu

Roll No. 800822013

Under the Guidance of:

Dr. Abhijit Mukherjee

(Director, Thapar University)

Ms. Shruti Sharma

(Assistant Professor, CED)

DEPARTMENT OF CIVIL ENGINEERING
THAPAR UNIVERSITY, PATIALA-147004, INDIA
JULY- 2010

CERTIFICATE

This to certify that the work presented in this thesis titled "**Monitoring of damage in pre-stressing tendons using ultrasonic guided waves** " being submitted by **Naveen Sachu** in partial fulfillment of requirements for the award of degree of Master of Engineering in Structural Engineering, at Civil Engineering Department, Thapar University, Patiala is an authenticated record of the initial work carried out by him under the supervision of **Dr. Abhijit Mukherjee, Director**, Thapar University, Patiala and **Ms. Shruti Sharma, Assistant Prof., CED,** Thapar University, Patiala.

The matter embodied in this report has not been submitted in parts or full to any other university or institute for the award of any degree.

Dr. Abhijit Mukherjee
Director
Thapar University, Patiala

Ms. Shruti Sharma
Assistant Prof., CED
Thapar University, Patiala

Countersigned by:

Dr. Maneek Kumar
Professor & Head, CED
Thapar University, Patiala

29/7/10
Dr. R. K. Sharma
Dean, Academic Affairs
Thapar University, Patiala

ACKNOWLEDGEMENT

I take this opportunity to express my sincere gratitude to **Dr. Abhijit Mukherjee, Director**, Thapar University for giving me the opportunity of doing my thesis work under his guidance. I am also thankful to him for his constant supervision and valuable suggestions.

It is my proud privilege to express regards and sincere gratitude to **Ms. Shruti Sharma, Assistant Professor,** Civil Engineering Department, Thapar University, Patiala, for her patient listening of my ideas and also suggesting new ways for implementing my ideas by her expert guidance throughout my work.

I am also thankful to **Dr. Maneek Kumar, Head Civil Engineering Department,** Thapar University, Patiala, for the motivation and inspiration that triggered me for the thesis work.

I also take this opportunity to thank to the entire faculty and staff of **Civil Engineering Department,** Thapar University, Patiala, for their help, inspiration and moral support, which went a long way in successfully completion of this report.

Finally, I want to acknowledge all the little help that I constantly received from Surinder Pal, Dynamics Lab helper and my colleagues, Bhavneet Kaur, Gurjot Singh and many more.

Naveen Sachu

(Roll No. 800822013)

ABSTRACT

One of the most common constructions nowadays is Pre-stressed Concrete structures. But due to deterioration of tendons caused by corrosion in concrete/grout, catastrophic collapses of Pre-stressed concrete constructions have been observed. Thus, a rigorous inspection of the embedded tendons in PSC for corrosion related damages on a regular basis is imperative. In the present work, high frequency ultrasonic guided waves have been utilized to develop a damage detection methodology for tendons embedded in concrete corrosion of simulated notch and debond defects. Conventional techniques of pulse transmission and pulse echo techniques are for testing. The time of flight in P/E and signal attenuation in both P/E and P/T have been observed to locate and quantify damages accurately. The method is then successfully applied to reinforced concrete beam specimens with embedded tendons undergoing accelerated chloride corrosion. Ultrasonic guided waves have been identified as a potentially effective technique for monitoring tendon corrosion in concrete. Suitable surface and core seeking ultrasonic guided wave modes have been identified which are sensitive to delamination and pitting effects of corrosion respectively. These modes are used to ultrasonically monitor reinforced concrete beams undergoing accelerated impressed current corrosion in chloride environment. The simulated and actual corrosion results are compared to show suitability of simulated techniques. The ultrasonic signals effectively relate to the state of pre-stressing tendon undergoing actual corrosion. Tendon in concrete results in pitting of tendons and debonding from surrounding grout. Hence, it is simulated in the form of notches (represents area loss) and delamination (represents debonding).

Hence, it is concluded that ultrasonic guided waves can be utilized for onsite inspection of embedded tendons for any breaks/cracks in tendons and corrosion related damages. Certain practical issues have to be looked into before it can be successfully developed into a fully fledged monitoring system.

CONTENTS

LIST OF FIGURES

LIST OF TABLES

CHAPTER 1

INTRODUCTION

1.1 GENERAL

Pre-stressed concrete is one of the most common construction materials used nowadays. It is a well-established fact that the basic economy of pre-stressed concrete lies in its high strength to weight and strength to cost ratios, its resistance to fire and cracking, and its versatility and adaptability. Pre-stressed concrete is ideally suited for long-span bridge construction. Pre-stressed concrete structures fall in two categories of pre-tensioned and post-tensioned constructions. Post-tensioned concrete is commonly used for long span bridge constructions where dead weights are large. It combines efficient use of concrete and steel with durability and speed of construction. Segmental post-tensioned superstructures are particularly favorable alternatives for long spans and for construction in areas where minimal disruption of the environment is required. Over a period of time, the high tension steel (tendon) is subjected to over stress and environmental degradation due to which defects/cracks occurs. If the damage goes unnoticed, it can lead to catastrophic failures. Hence, monitoring of damage in the embedded tendons is of prime importance.

1.2 MATERIALS FOR PRE-STRESSED CONCRETE

Materials used in pre-stressed concrete members are high strength concrete and high tensile steel. The significant observations which resulted from the pioneering research on pre-stressed concrete were:

- Necessity of using high-strength steel and concrete.
- Recognition of losses of pre-stress due to various causes.

1.2.1 High-strength concrete

Stronger concrete is usually required for pre-stressed than for reinforced work. Present practice in this country calls for 28 day cylinder strength of 28-55MPa for pre-stressed concrete, while

the corresponding value for reinforced concrete is around 24MPa. The usual cube strength specified for pre-stressed concrete in Europe is about 450kg/cm^2, based on 10-, 15-, or 20-cm cubes at 28 days. High-strength concrete is necessary in pre-stressed concrete, as the material offers high resistance in tension, shear, bond and bearing. In the zone of anchorages, the bearing stresses being higher, high-strength concrete is invariably preferred to minimize costs. High strength concrete is less liable to shrinkage cracks, and has a higher modulus of elasticity and smaller ultimate creep strain, resulting in a smaller loss of pre-stress in steel. The use of high-strength concrete results in a reduction in the cross-sectional dimensions of pre-stressed concrete structural elements. With a reduced dead-weight of the material, longer spans become technically and economically practicable.

1.2.2 High-tensile steel

The early attempts to use mild steel in pre-stressed concrete were not successful, as a working stress of 120 N/mm^2 in mild steel is more or less completely lost due to elastic deformation, creep and shrinkage of concrete. The normal loss of stress in steel is generally about 100 to 240 N/mm^2 and it is apparent that if this loss of stress is to be a small portion of the initial stress, the stress in steel in the initial stages must be very high, about 1200 to 2000 N/mm^2. These high stress ranges are possible only with the use of high-strength steel.

For Pre-stressed concrete members, the high-tensile steel used generally consists of wires, bars, or strands **(Fig.1.1 (a) & (b))**. The higher tensile strength is generally achieved by marginally increasing the carbon content in steel in comparison with mild steel. High-tensile steel usually contains 0.6 to 0.85 per cent carbon, 0.7 to 1 per cent manganese, 0.05 per cent of sulphur and phosphorus with traces of silicon. The high-carbon steel ingots are hot-rolled into rods and cold-drawn through a series of dies to reduce the diameter and increase the tensile strength. The process of cold-drawing through dies decreases the durability of the wires. The cold-drawn wires are subsequently tempered to improve their properties. Tempering or ageing or stress relieving by heat treatment of the wires at 150-420^{o}C enhances the tensile strength. The cold-drawn stress relieved wires are generally available in nominal sizes of 2.5, 3, 4, 5, 7 and 8 mm diameter. The hard-drawn steel wires which are indented or crimped are preferred for pre-tensioned elements because of their superior bond characteristics. The small diameter wires of 2 to 5 mm are mostly used in the form of strands comprising two, three or seven wires. The helical form of twisted

wires in the strands substantially improves the bond strength. Two-and 3-ply strands are made up of 2 mm and 3 mm diameter individual wires, while the 7-ply strands are twisted using wires of 2 to 5 mm diameter. The nominal diameter of 7-ply strands varies from 6.3 mm to 15.2 mm. The high-tensile steel bars commonly employed in pre-stressing are manufactured in nominal sizes of 10, 12, 16, 20, 22, 25, 28 and 32 mm diameter. The ultimate tensile strength of the bars does not vary appreciably with the diameter, since the high strength of the bars is due to alloying rather than to cold working as in the case of wires. The British standard code **BS: 2691**, **BS: 4486** and **BS: 3671** present specifications for the use of 19 wire strands in addition to the earlier 7-wire strands.

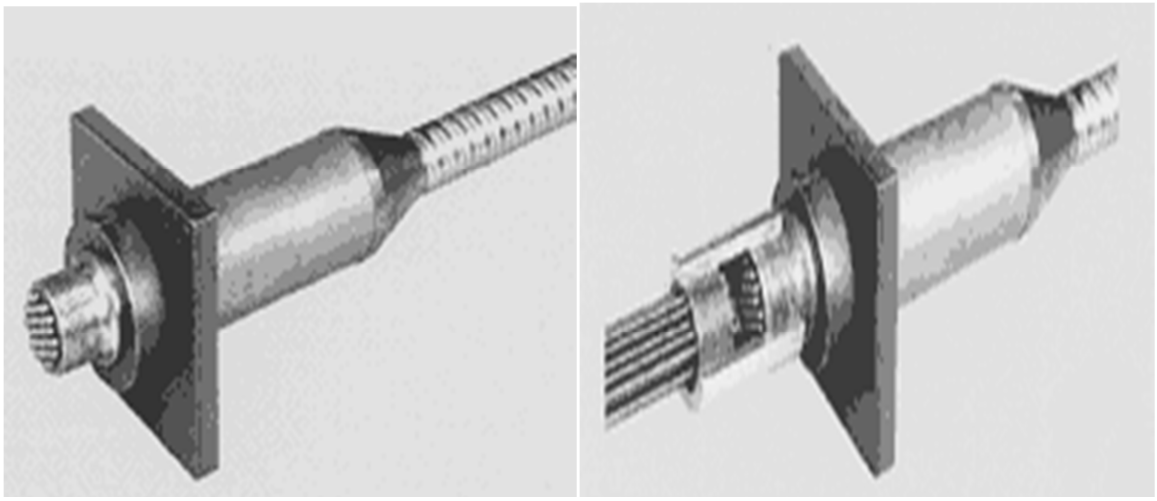

(a) B.B.R.V. Wire Tendon with Button Heads

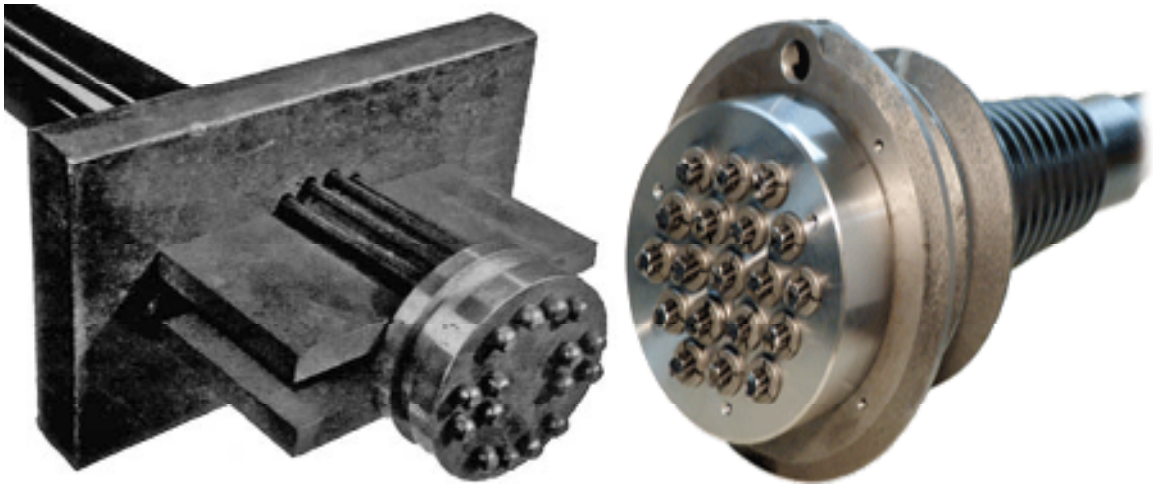

(b) B.B.R.V. Strand Tendon

Fig.1.1 [Google images]

1.2.2.1 Types of pre-stressing steel

The development of pre-stressed concrete was influenced by the invention of high strength steel. It is an alloy of iron, carbon, manganese and optional materials. The following material describes the types and properties of pre-stressing steel. In addition to pre-stressing steel, conventional non-pre-stressed reinforcement is used for flexural capacity (optional), shear capacity, temperature and shrinkage requirements.

Wires

A pre-stressing wire is a single unit made of steel. The nominal diameters of the wires are 2.5, 3.0, 4.0, 5.0, 7.0 and 8.0 mm. The different types of wires are as follows.

1) Plain wire: No indentations on the surface.
2) Indented wire: There are circular or elliptical indentations on the surface.

Strands

A few wires are spun together in a helical form to form a pre-stressing strand. The different types of strands are as follows.

1) Two-wire strand: Two wires are spun together to form the strand.
2) Three-wire strand: Three wires are spun together to form the strand.
3) Seven-wire strand: In this type of strand, six wires are spun around a central wire. The central wire is larger than the other wires.

Tendons

A group of strands or wires are placed together to form a pre-stressing tendon. The tendons are used in post-tensioned members. The following figure shows the cross section of a typical tendon. The strands are placed in a duct which may be filled with grout after the post-tensioning operation is completed **(Fig. 1.2)**.

Cables

A group of tendons form a pre-stressing cable. The cables are used in bridges.

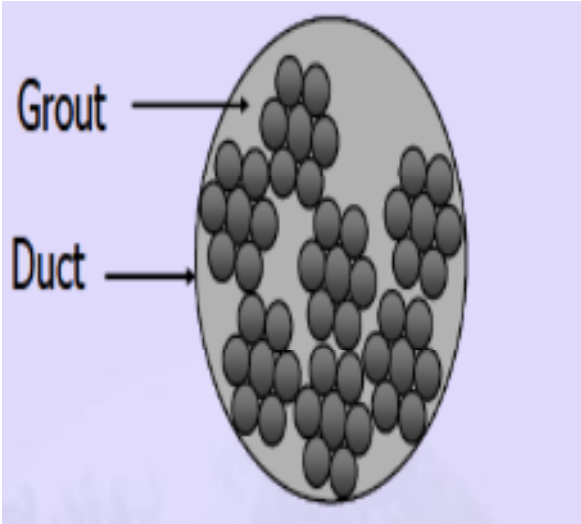

Fig.1.2 Cross-section of a typical tendon [Amlan et al. (section 1.7)]

Bars

A tendon can be made up of a single steel bar. The diameter of a bar is much larger than that of a wire. Bars are available in the following sizes: 10, 12, 16, 20, 22, 25, 28 and 32 mm.

The following **(Fig.1.3)** shows the different forms of pre-stressing steel.

Fig.1.3 Forms of reinforcing and pre-stressing steel [Amlan et al. (section 1.7)]

1.2.2.2 Properties of pre-stressing steel

The steel in pre-stressed applications has to be of good quality. It requires the following attributes.

(1) High strength

(2) Adequate ductility

(3) Bendability, which is required at the harping points and near the anchorage

(4) High bond, required for pre-tensioned members

(5) Low relaxation to reduce losses

(6) Minimum corrosion.

Tensile strength of pre-stressing steel

The tensile strength of pre-stressing steel is given in terms of the characteristic tensile strength (f_{pk}). The characteristic strength is defined as the ultimate tensile strength of the coupon specimens below which not more than 5% of the test results are expected to fall.

The ultimate tensile strength of a coupon specimen is determined by a testing machine according to **IS: 1521 - 1972**, Method for Tensile Testing of Steel Wire. The following **(Fig.1.4)** shows a test setup.

(a) Test set-up

(b) Failure of a strand

Fig.1.4 Testing of tensile strength of pre-stressing strand [Amlan et al. (section 1.7)]

The minimum tensile strengths for different types of wires as specified by the codes are reproduced in **Table1.1**.

Table1.1 Cold Drawn Stress-Relieved Wires (IS: 1785 Part 1)

Nominal Diameter (mm)	2.50	3.00	4.00	5.00	7.00	8.00
Minimum Tensile Strength (f_{pk}) (N/mm^2)	2010	1865	1715	1570	1470	1375

The proof stress (defined later) should not be less than 85% of the specified tensile strength.

Table1.2 As-Drawn wire (IS: 1785 Part 2)

Nominal Diameter (mm)	3.00	4.00	5.00
Minimum Tensile Strength (f_{pk}) (N/mm^2)	1765	1715	1570

The proof stress should not be less than 75% of the specified tensile strength.

Table1.3 Indented wire (IS: 6003)

Nominal Diameter (mm)	3.00	4.00	5.00
Minimum Tensile Strength (f_{pk}) (N/mm^2)	1865	1715	1570

The proof stress should not be less than 85% of the specified tensile strength.

For high tensile steel bars (**IS: 2090**), the minimum tensile strength is 980 N/mm^2. The proof stress should not be less than 80% of the specified tensile strength.

Stress-strain curves for pre-stressing steel

The stress versus strain behaviour of pre-stressing steel under uniaxial tension is initially linear (stress is proportional to strain) and elastic (strain is recovered at unloading) **(Fig.1.5)**. Beyond about 70% of the ultimate strength the behaviour becomes nonlinear and inelastic. There is no defined yield point. The yield point is defined in terms of the proof stress or a specified yield strain. **IS:1343 - 1980** recommends the yield point at 0.2% proof stress. This stress corresponds to an inelastic strain of 0.002 **(Fig.1.5)**. The characteristic stress-strain curves are given in **(Fig.1.6)** of **IS:1343 - 1980**.

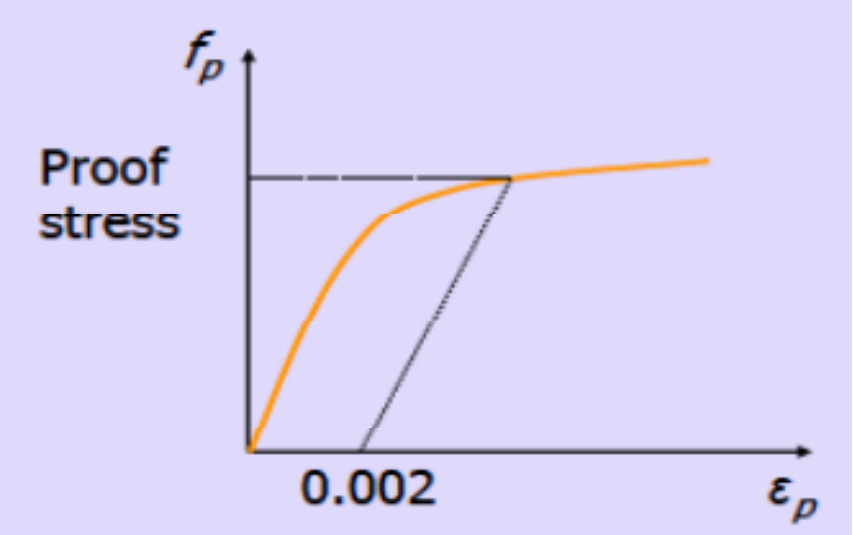

Fig.1.5 Proof stress corresponds to inelastic strain of 0.002

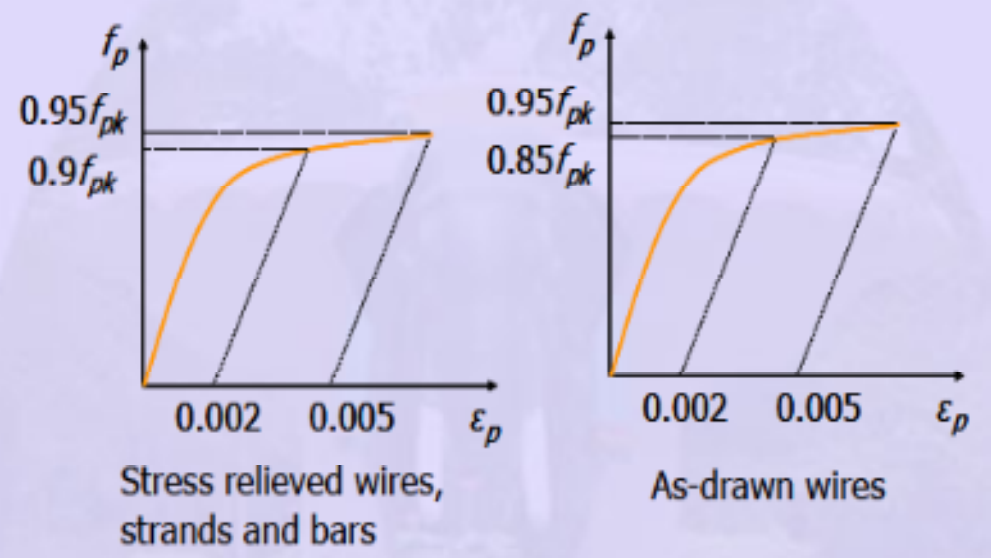

Fig.1.6 Characteristic stress-strain curves for pre-stressing steel

(Fig.1.6, IS:1343 - 1980)

The stress-strain curves are influenced by the treatment processes. **(Fig.1.7)** shows the variation in the 0.2% proof stress for wires under different treatment processes.

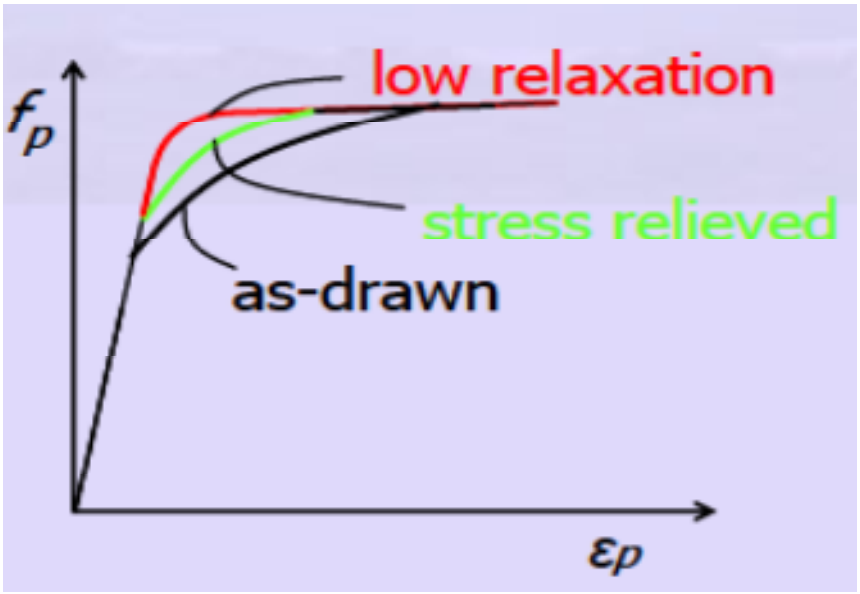

Fig.1.7 Variation in the 0.2% proof stress for wires under different treatment processes

The design stress-strain curves are calculated by dividing the stress beyond $0.8f_{pk}$ by a material safety factor γ_m =1.15. **(Fig.1.8)** shows the characteristic and design stress-strain curves.

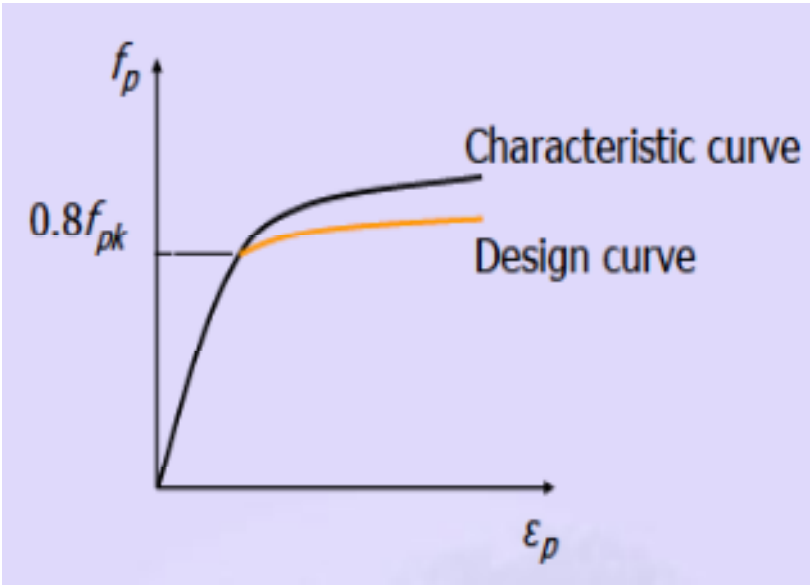

Fig.1.8 Characteristic and design stress-strain curves for Pre-stressing steel [Amlan et al. (section 1.7)]

1.3 NEED FOR MONITORING TENDONS OF PSC MEMBERS

There is a need for non-invasive, in-situ and real time corrosion monitoring system for embedded reinforcing strands that could identify the nature and extent of corrosion undergone by the structure. The pre-stressing steel has the following two major detrimental effects on the durability of structures:

(1) Corrosion
(2) Cracks/Fracture

1.3.1 Corrosion of tendons/pre-stressing steel

Corrosion of pre-stressing steel in concrete leading to premature damage to concrete structures is a multibillion dollar problem prevalent all over the world. Corrosion-related damage to bridge structures which requires costly repairs is the single most challenging issue for most highway agencies. It is worthwhile to understand the fundamentals of corrosion theory to gain a deeper perspective of the current problems in the concrete industry pertaining to corrosion-related issues.

1.3.1.1 Corrosion chemistry

An understanding of a general corrosion theory for metals is necessary prior to considering the corrosion of pre-stressing steel in concrete. Corrosion of iron is an electrochemical process (equations 1.1 and 1.2), commonly known as half-cell reactions:

$$Fe \rightarrow Fe^{2+} + 2e^{-} \qquad \text{(anodic half-cell reaction)} \qquad (1.1)$$

$$2H_2O + O_2 + 4e^{-} \rightarrow 4OH^{-} \qquad \text{(cathodic half-cell reaction)} \qquad (1.2)$$

Electrochemical oxidation takes place at the anode and reduction at the cathode. Both the electrodes form on the metal surface. Iron is oxidized into ferrous ions at the anode as shown by

eqn1. The ferrous ions are converted to 2Fe $(OH)_3$ through a series of reactions and produce rust. The formation of rust can be understood from following equations.

$$2Fe + 2H_2O + O_2 \rightarrow 2Fe^{2+} + 4OH^- \rightarrow 2Fe(OH)_2. \quad (1.3)$$

Ferrous hydroxide can react further to yield ferric salt or the popular rust:

$$2Fe(OH)_2 + 2H_2O + O_2 \rightarrow 2Fe(OH)_3 \quad (1.4)$$

The anodic and cathodic areas are regions of different electrochemical potential that develop due to two different metals (which therefore have different potentials) or a single metal with surface differences that could be metallurgical or local variations in electrolyte. The anode and cathode locations can change often and have an irregular pattern leading to a somewhat uniform corrosion or the locations can be more fixed and localized.

The cement paste pore solution acts as an electrolyte and anodes and cathodes are formed on the steel surface when corrosion of steel in concrete commences. The basic corrosion process is shown in **(Fig.1.9)**.

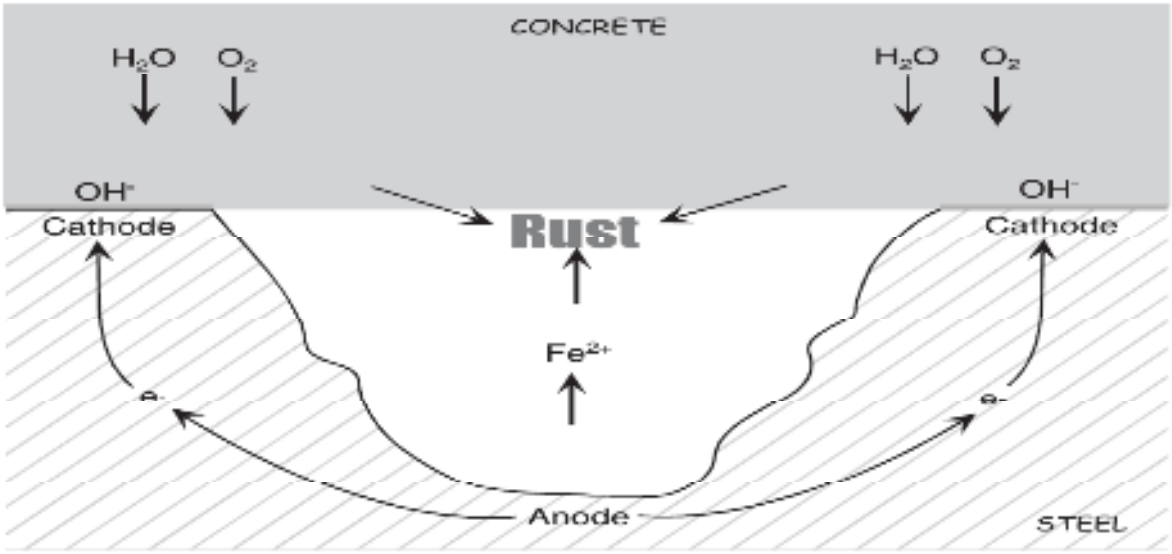

Fig.1.9 Corrosion of steel in concrete [Iyer et al. (2002)]

The high alkalinity of the grout (or concrete in traditionally reinforced systems) provides a protective environment for the reinforcing steel. An oxide film develops on the steel protecting it

from corrosion. Chlorides break down this passive layer in spots and begin the corrosion process. Areas where the film has broken down are anodes and those with film remaining are cathodes. Pitting corrosion occurs at the anodes and high cathode-to-anode ratio further speeds up the corrosion process. If the alkaline (high pH) environment is lost, the steel is susceptible to corrosion.

1.3.1.2 Corrosion of pre-stressing steel

The steel used in pre- and post-tensioned concrete is prone to corrosion attacks due to chloride induced corrosion, and theoretically would be susceptible to stress corrosion cracking (SCC) or hydrogen embrittlement (HE). Chloride-induced corrosion is the most common form of corrosion in pre-stressed concrete. It can be relatively quick and can localize to cause significant reductions in cross-sectional area. The concrete surface is stained due to the rust produced which also causes cracking and spalling. Corrosion is dependent on several variables and hence controversial views exist regarding chloride thresholds. These variables are: proportioning of concrete, type and specific area of cement, water-cement ratio, sulfate content, curing conditions, age, environment, carbonation, type and condition of reinforcement, temperature and relative humidity.

Uniform corrosion is a generalized corrosion over large area. This type of corrosion may result in large amount of metal loss, but does not cause localized damage and hence a catastrophic failure is less likely to occur as compared to other types of corrosion. Pitting, as typically seen on steel in a high pH environment, is a form of extremely localized attack that results in pits in the metal. Pits may be small or large in diameter, but in most cases are relatively small. Pitting is one of the most destructive and insidious forms of corrosion. Pitting corrosion is very common in pre-stressed concrete structures and can be quite destructive due to the concentrated pits of corrosion causing large reductions in cross-sectional area with a small amount of overall metal loss. The process is a self-propagating one. As the pits grow, the surface can be undercut resulting in a deceivingly large pit making detection difficult even on bare steel.

Cross-sectional geometry of the steel along with high strength and high tensile loadings make a post-tensioned structure a possible candidate for catastrophic failure if chlorides are allowed easy access to the strand. Proper grouting of the post-tensioning ducts is necessary for corrosion

protection and bond transfer, but complete grouting can be difficult due to lack of visibility and access to all parts of the duct. A survey of post-tensioned bridges in all over the world indicates that although most of the bridges were satisfactory and in acceptable condition, the majority of post-tensioning ducts were inadequately injected with grout. In some cases, the ducts had been left completely ungrouted. Schupack examined a 35-year-old post-tensioned bridge and found similar problems with ducts. Many of the tendons inspected were either partially grouted or left ungrouted. The grout water-cement ratios varied through the span and in some spans, chloride-contaminated grout had been used.

The grout injected into post-tensioned ducts serves a dual role of providing bonding between concrete and the pre-stressing steel as well as protecting the steel from corrosion. Segregation of cement and water may lead to accumulation of bleed water at high points in the tendon profile while the grout is still plastic. As grout sets, bleed water may also collect at intermediate points in very tall grout columns or on top of horizontal pre-stressing steel. This phenomenon can result in voids in the duct and anchorage area leading to possible corrosion of tendon.

The anchorage zone in a post-tensioned structure or the end anchor of the post-tensioning tendons is a sensitive part of its integrity. Hence the tendons in this region must be protected properly to reduce their vulnerability to corrosion-encouraging agents. Post-tensioning cables tend to be inaccessible to visual inspection, so that corroding tendons may go unnoticed for long periods of time. The potential problem areas can thus be avoided through thoughtful planning, monitoring and periodic inspection.

1.3.2 Cracks / fractures in tendons

The importance of cracks in accelerating corrosion by allowing access of corrosion agents to the steel surface has been widely discussed. If pre-stressing steel is doing its job in areas of tension in the structure, small cracks will occur as the tensile load exceeds the tensile strength of the steel. Most of these are small cracks (<0.5mm) at right angles to the pre-stressing steel. They should not significantly affect the rate of corrosion of the steel as any local ingress of chlorides, moisture and carbonation is limited and contained by the local alkanity. Obviously there is a limit to this self healing ability. If there are large cracks that stay open (>0.5mm), or excessive shrinkage cracks along the bars then corrosion can be accelerated. Corrosion causes horizontal

cracking along the plane of the rebar and the corner cracking around the end rebar. This leads to the loss of concrete cover **(Fig.1.10)**.This is the main consequences of reinforcement corrosion with its subsequent risk of falling concrete and unacceptable appearance.

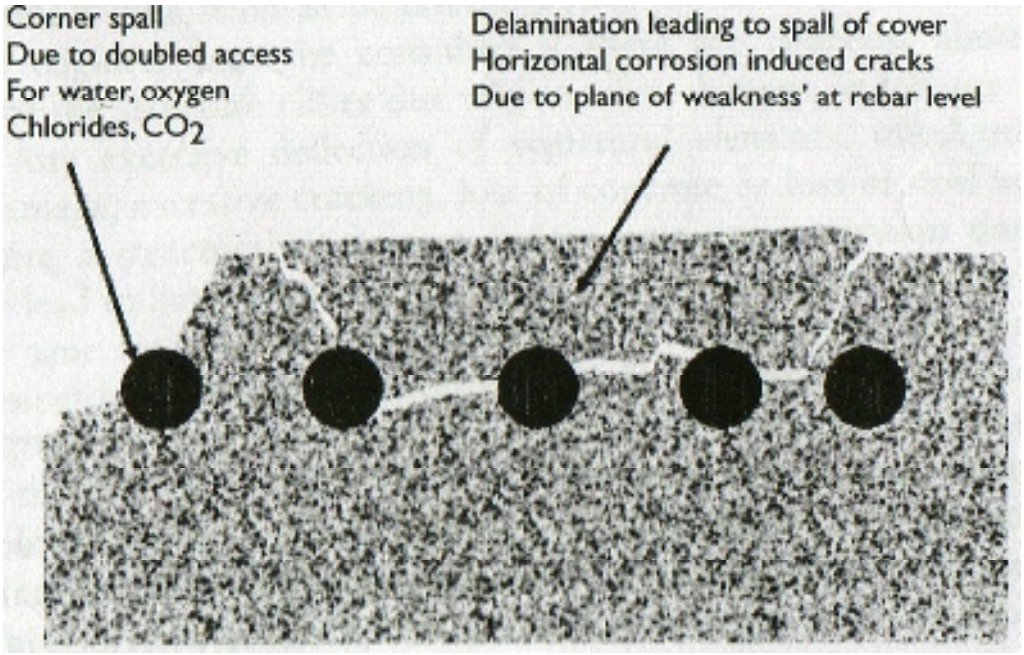

Fig.1.10 Schematic of corrosion induced spalling at corners and delamination at the plane of the reinforcement [Broomfield et al. (2002)]

1.3.2.1 Stress corrosion cracking (SCC)

The phenomenon of stress corrosion in steel is particularly dangerous, as it results in sudden brittle fractures. Stress-corrosion cracking results from the combined action of corrosion and static tensile stress, which may be either residual or externally applied. This type of attack in alloys is due to the internal metallurgical structure, which is influenced by composition, heat treatment and mechanical processing. The causes of the susceptibility of high-tensile steels to stress corrosion are manifold. Heat-treated wires are especially prone to stress-corrosion fractures when compared to drawn wires. If the ducts of post-tensioned members are not grouted, there is a possibility of stress corrosion leading to a catastrophic / failure of the structure. Other common types of corrosion frequently encountered in pre-stressed concrete constructions are pitting corrosion and chloride corrosion. Some of the important protective measures against

stress corrosion include protection from chemical contamination, protective coatings for high-tensile steel and grouting of ducts immediately after pre-stressing operations.

1.3.2.2 Hydrogen embrittlement (HE)

Atomic hydrogen is liberated as a result of the action of acids on high-tensile steels. This penetrates into the steel surface, making it brittle and fracture-prone on being subjected to tensile stress. Even small amounts of hydrogen can cause considerable damage to the tensile strength of high-tensile steel wires. Use of high-alumina cement and blast-furnace-slag cement, which are rich in sulphides, for making pre-stressed concrete can cause hydrogen embrittlement. Use of dissimilar metals, such as aluminums and zinc for sheaths to house high tensile steel wires, also results in hydrogen embrittlement. Similarly, minute traces of sulphur, which come in contact with high-tensile steel wires in the presence of moisture, can drastically reduce their strength.
In order to prevent hydrogen embrittlement, it is essential that the steel is properly protected from the action of acids. Protective coverings like bituminous crepe-paper covering during transport, reduces the chances of contamination. The wires should be protected from rain water and excessive humidity by storing them in dry conditions.

1.4 DAMAGE DETECTION METHODS

Essential structural elements for the safety, serviceability and durability of pre-stressed concrete structures are the post-tensioning tendons. It is desirable to reliably assess their behavior in existing structures. The most ideal way of attaining this objective is to perform nondestructive or at least low-destructive inspection methods that cause minimum disturbance to the user. These methods help us detect possible defects or damage such as grout voids or tendon corrosion. A few non- or low-destructive inspection and monitoring methods are discussed below that either detect existing grout voids, corrosion of the pre-stressing steel in progress or even ruptured wires, strands or bars in tendons.

1.4.1 NON DESTRUCTIVE TESTING METHODS (NDT)

The field of Nondestructive testing (NDT) is a very broad, interdisciplinary field that plays a critical role in assuring that structural components and systems perform their function in a

reliable and cost effective fashion. The term is generally applied to investigations of material integrity. These tests are performed in a manner that does not affect the future usefulness of the object or material. Because it allows inspection without interfering with a product's final use, NDT provides an excellent balance between quality control and cost-effectiveness.
Nondestructive evaluation (NDE) is another term that is often used interchangeably with NDT. However, technically, NDE is used to describe measurements that are more quantitative in nature. For example, a NDE method would not only locate a defect, but it would also be used to measure something about that defect such as its size, shape, and orientation. NDE may be used to determine material properties such as fracture toughness, formability, and other physical characteristics.

1.4.2 VARIOUS METHODS OF NDT

Although a number of different NDT methods have been developed, but following methods are most commonly used.

• **IMPACT ECHO METHOD:** The impact-echo method is a technique for flaw detection in concrete. It is based on monitoring the surface motion resulting from a short-duration mechanical impact. The method overcomes many of the barriers associated with flaw detection in concrete based on ultrasonic methods. It can be used to check a tendon for pre-stressed grout voids but is a delicate operation requiring skilled personnel. The presence of cracks and other concrete defects as often found in real structures influences significantly the test results and can make the evaluation impossible at times.

• **REMNANT MAGNETISM METHOD:** This method developed in Germany detects fractures in steel. The magnetizing and recording equipment has to be moved along the tendon path on auxiliary guidance rails and scaffolding fixed to the concrete surface in order to measure a magnetic leakage field generated by the formation of magnetic dipole distribution around the fracture area. Fracture patterns have typical signatures that are matched and interpreted by experienced personal or pattern recognition (PR) software. The method is suitable to locate fractures of steel strands and to detect real corrosion. But the major constraint of this method is

the difficulty in coping with the disturbing magnetic signals originating from other embedded steel elements such as normal reinforcement, anchorage elements, duct couplers, steel plates, nails, etc.

• **REFLECTOMETRICAL IMPULSE MEASUREMENT (RIMT):** RIMT employs time-domain reflectometry to locate anomalies such as corrosion, breakage of wires or whole tendons. It involves the sending of a high-frequency impulse along a tendon or anchor and allows in-situ measurement of the integrity of steel and rock/soil anchors. This method is expensive and incomplete because it requires the destruction and restoration of a part of the structure. Also the recorded signals do not contain information on the condition of the tendon but are artifacts of the measurement procedure. Thus, Matt disregards it as a diagnostic technique for grouted tendons.

• **VISUAL AND OPTICAL TESTING:** Visual inspection involves using an inspector's eyes to look for defects. The inspector may also use special tools such as magnifying glasses or mirrors gain access and more closely inspect the subject area.

• **RADIOGRAPHY (RT):** Radiography involves the use of penetrating gamma or X-radiation to examine parts and products for imperfections. An X-ray generator or radioactive isotope is used as a source of radiation. The resulting shadowgraph shows the dimensional features of the part. Possible imperfections are indicated as density changes on the film in the same manner as medical X-ray shows broken bones.

• **THERMOGRAPHY:** All objects naturally emit infrared radiation in proportion to their surface temperature. Thermography measures the emitted radiation and displays the information as a visual image. By combining infrared and computer technologies, it is possible to generate thermo grams (heat pictures), having up to 256 colors, that clearly show thermal profiles and temperature measurements. A combination of thermography and natural heating/cooling cycle allows areas of delaminated concrete and debonded tendons to be detected. The advantages of this technique are that it is a remote operation and is nondestructive.

• **TOMOGRAPHY:** Acoustic tomographic imaging of concrete is a developing nondestructive evaluation technology and has a potential to assess the condition of concrete structures. Although this technology has been used with great success to image fluid-rich media like biological tissue, the complex behavior of stress waves in solids complicates the imaging of concrete, masonry and other heterogeneous materials such as those used to construct concrete structures.

• **ACOUSTIC EMISSION TESTING (AE):** When a solid material is stressed, imperfections within the material emit short bursts of acoustic energy called "emissions." as in ultrasonic testing; acoustic emissions can be detected by special receivers. Emission sources can be evaluated through the study of their intensity, rate, and location.

• **ULTRASONIC TESTING (UT):** Ultrasonic testing use transmission of high-frequency sound waves into a material to detect imperfections or to locate changes in material properties. The most commonly used ultrasonic testing technique is pulse echo, wherein sound is introduced into a test object and reflections (echoes) are returned to a receiver from internal imperfections or from the part's geometrical surfaces.

1.5 ULTRASONIC TESTING (UT)

Ultrasonic Nondestructive Testing introduces high frequency sound waves into a test object to obtain information about the object without altering or damaging it in any way. A typical UT inspection system consists of several functional units, such as the pulser/receiver, transducer, and display devices **(Fig.1.11)**. A pulser/receiver is an electronic device that can produce high voltage electrical pulses. Driven by the pulser, the transducer generates high frequency ultrasonic energy. The sound energy is introduced and propagates through the materials in the form of waves. When there is a discontinuity (such as a crack) in the wave path, part of the energy will be reflected back from the flaw surface. The reflected wave signal is transformed into an electrical signal by the transducer and is displayed on a screen.

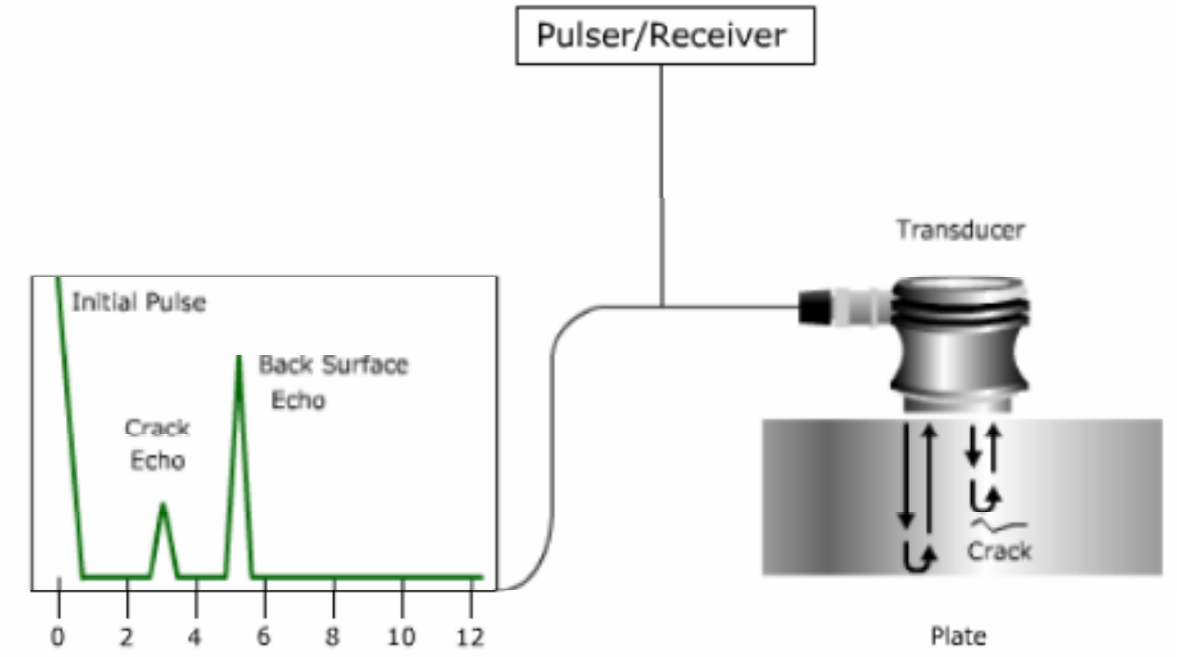

Fig.1.11 General ultrasonic Inspection Principle [Vermani et al. (2008)]

1.5.1 METHODS OF ULTRASONIC TESTING

(1) PULSE ECHO METHOD

(2) PULSE TRANSMISSION METHOD

- **PULSE ECHO METHOD**

In the pulse-echo method, a piezoelectric transducer with its longitudinal axis located perpendicular to and mounted on or near the surface of the test material is used to transmit and receive ultrasonic energy. The ultrasonic waves are reflected by the opposite face of the material or by discontinuities, layers, voids, or inclusions in the material, and received by the same transducer where the reflected energy is converted into an electrical signal. The electrical signal is computer processed for display on a video monitor or TV screen. The display can show the relative thickness of the material, depth into the material where flaws are located, and (with proper scanning hardware and software), where the flaws are located in the X-Y plane.

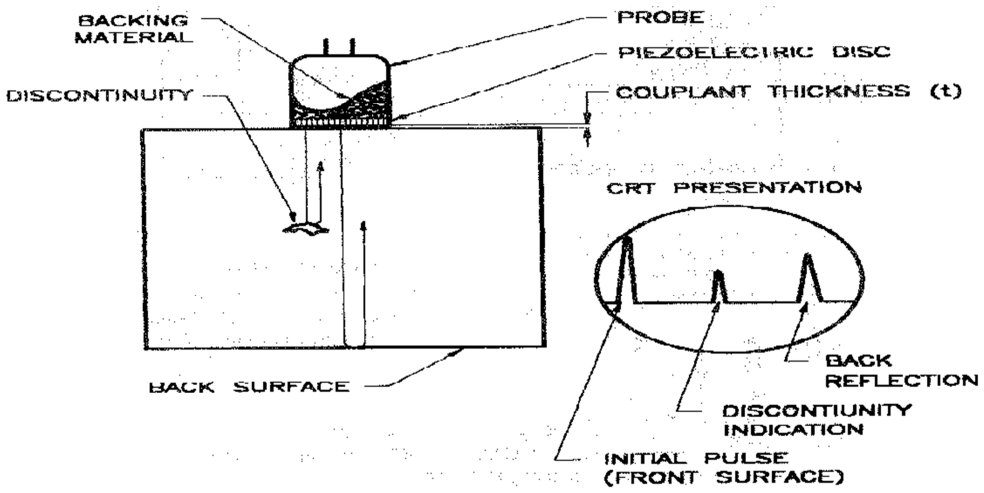

Fig.1.12 Principle of pulse echo method of inspection [Bindal]

- **PULSE TRANSMISSION METHOD**

In the pulse-transmission method, an ultrasonic transmitter is used on one side of the material while a detector is placed on the opposite side. One unit acts as transmitter and the other unit as receiver. The beam from the transmitter T travels through the material to its opposite surface where the receiving transducer R is placed. Scanning of the material using this method will result in the location of defects, flaws, and inclusions in the X-Y plane.

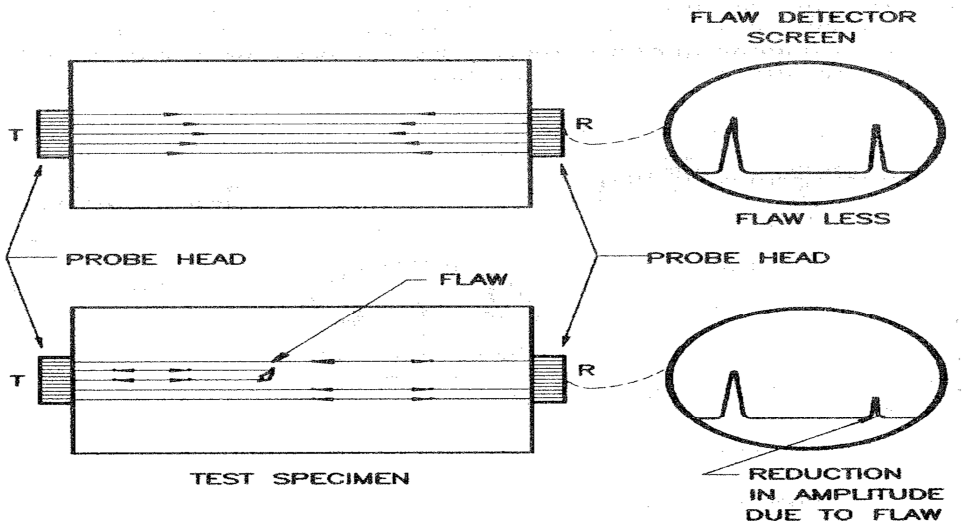

Fig.1.13 Principle of through transmission of ultrasonic testing [Bindal]

1.6 ULTRASONIC GUIDED WAVES FOR NON DESTRUCTIVE TESTING (NDT)

There are a family of guided or travelling waves which propagate in-plane, such as Raleigh, Lamb and interface waves. They are attractive for testing because they can propagate over long distances, allowing a line rather than a point to be interrogated. The Lamb wave can propagate a long distance along the reinforcing steel bars embedded in concrete as the guided wave and is sensitive to the interface bonding condition between the steel bar and the concrete. Bulk waves can only exist in an unbounded bulk of material. However, in structures with finite boundaries, such as a tendon, guided waves are formed that have more complicated properties than bulk waves.

The main difference between bulk and guided waves is that bulk waves travel in the bulk of the material (away from the boundaries) and guided waves travel either at boundaries (Surface waves) or between the boundaries (Lamb waves). Bulk and guided waves behave differently but they are actually governed by the same set of partial differential wave equations. The difference in the mathematical solution of the two types of waves is due to the boundary conditions. In the case of bulk waves, there is no need for boundary conditions because the wave is assumed to travel inside the bulk of the material **(Fig.1.14 (a))**. In contrast guided waves are the result of the interaction occurring at the interface between two different materials **(Fig.1.14 (b))**. This interaction produces reflection, refraction and mode conversion between longitudinal and shear waves which can be predicted using appropriate boundary conditions.

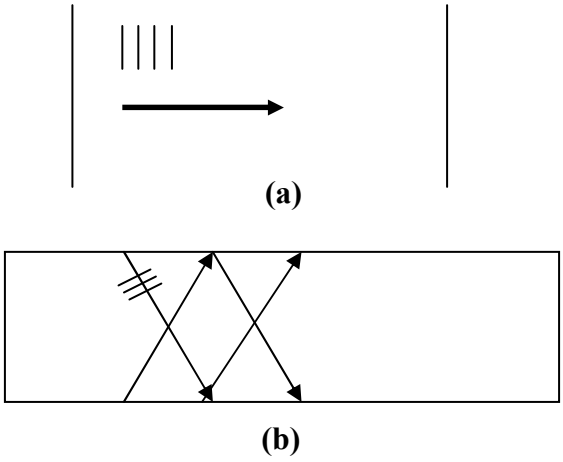

Fig.1.14 Schematic of (a) bulk wave and (b) guided wave [Kundu et al. (2003)]

1.7 CLOSING REMARKS

Various NDT methods can be used for damage detection of corrosion, fractures and other defecs in tendons. Either these techniques are too costly as they require skilled labour for their practical application or they suffer from drawbacks for inspection of grouted tendons. Ultrasonic guided waves can be explored as a potentially attractive option for defect detection in tendons. It is proposed in this work to estimate the suitability of longitudinal guided waves for monitoring of cracks/corrosion defects in tendons.

CHAPTER 2

LITERATURE REVIEW

This chapter presents a review of literature on utilization of ultrasonic waves for damage detection in reinforcing bars and tendons. It gives an idea of state of art of research. A summary of the work pertaining to the various methods for damage identification and inspection of tendons in structures can be classified based on the theoretical/analytical studies and experimental studies.

2.1 EXPERIMENTAL WORK DONE

The first part of the literature review is about the experimental studies carried out utilizing ultrasonic guided waves. A wide range of techniques have been reported in the literature that may be suitably employed for the monitoring of steel in concrete structures for the purpose of diagnosing the cause and extent of damage in the form of fractures and corrosion. **Li Yibo et al. (2006)** did experimental work on energy attenuation of ultrasonic guided waves going through girth welds. **Mukherjee et al. (2003)** worked on propagation through solids to locate the position and extent of crack with single actuator and several surface mounted sensors. **Mukherjee et al. (2005)** did the characterization of discretely graded materials using acoustic wave propagation. **He et al. (2006)** did the experimentation and said that the Guided waves can be used efficiently, both for measuring the length of a rod embedded in concrete and for estimating the amount of delamination between a steel rock bolt and concrete.

Lowe et al. (1998) presented the technique of wave propagation and their sensitivity to defects through pipes using pulse echo. Issues of importance were the selection of the optimum guided wave modes and the establishment of relationships between the defect size and the strength of wave reflection.

Kundu et al. (1998) studied the lamb wave propagation in large plates and its use in internal defect detection. The lamb wave modes which are most efficient for detecting different types of defects are identified. Stress fields inside the plate for different modes of lamb waves are

computed. From these stress plots, the most efficient mode for detecting the particular types of defect can be identified.

Kundu et al. (2001) investigated the difficulties in detection of internal defects in mirror symmetric composite plates using lamb wave modes. In a symmetrically layered composite plate stress, displacement magnitudes and energy distribution profiles for all lamb modes are symmetric about central plane of the plate. As a result, ability of lamb mode to detect a defect in corresponding layer of mirror symmetry. Hence form lamb wave image generated, its difficult to distinguish between the defects in two layers of mirror symmetry. The authors discuss to solve the problem by fine tuning of frequency used and striking angle of incident beam.

Iyer et al. (2002) proposed ultrasonic C-scan imaging to detect corrosion and voids in post-tensioning tendons. Investigations on post-tensioned specimens using ultrasound C-scan imaging technique have proved this method to be promising for future applications in the evaluation of corrosion and voids in post-tensioned tendons. But the study recommends further investigations to upgrade the technique from bench-top to a field-ready instrument.

Kundu et al. (2002) investigated the feasibility of detecting internal defects (cracks, honeycombs, and inclusions) in reinforced concrete (RC) beams using ultrasonic guided waves. Experiments were carried out on full-scale beams. It is shown that for RC beam inspections, the guided wave technique was better than the conventional stress wave techniques.

Kundu et al. (2003) studied the feasibility of detecting interface degradation and separation of steel bars in concrete beams using Lamb waves. The Lamb wave can propagate a long distance along the reinforcing steel bars embedded in concrete as the guided wave and is sensitive to the interface bonding condition between the steel bar and the concrete. The traditional ultrasonic methods for inspecting defects in concrete use reflection, transmission, and scattering of longitudinal waves by internal defects. This investigation shows that the Lamb wave inspection technique is an efficient tool for health monitoring of reinforced concrete structures.

Beard et al. (2003) states that there is currently a need to improve the nondestructive testing techniques that are used to inspect grouted steel reinforcing tendons, anchors, and rock bolts for corrosion and fracture. A method of inspection using guided ultrasonic waves has been proposed, which uses a pulse-echo technique carried out from the free end of the structure. The maximum inspection range is determined by the amount of attenuation that the wave experiences as a result of leakage into the embedding material and material losses. However, previous work has identified high frequency modes that have low attenuation and so increase the inspection range. Research has been carried out with a focus on the inspection of the post-tensioning tendons used to reinforce concrete. The research presented by uses experimental techniques to measure the attenuation in short lengths of grouted tendons, to evaluate the reflection coefficient of the modes from different geometry breaks, and to assess the impact of tendon curvature. The outcome of this research shows that the inspection range for tendons is limited, but the outlook for the inspection of the larger diameter grouted bolts and rebars that are used in the construction industry is promising. Considerable success has already been achieved in the testing of epoxy bonded rock bolts using this method.

Paul et al. (2004) studied the sensitivity of corrosion and fatigue damage detection using Guided ultrasonic waves. Guided waves have stress distributed through the thickness of the structure and can propagate over large distances. At structural defects, e.g. severe thickness reduction due to corrosion pitting, the guided wave mode is scattered and part of its energy reflected back towards the monitoring location. This allows for the efficient nondestructive testing and monitoring of large technical structures. A guided ultrasonic waves array, consisting of piezoelectric transducer elements for the excitation and reception of the first antisymmetric lamb wave mode Ao was designed and built. Laboratory measurements for a steel plate containing various defects were performed and results compared to theoretical predictions.

Iyer et al. (2005) described that assessing the condition of underground pipelines such as water lines, sewer pipes, and telecommunication conduits in an automated and reliable manner is vital to the safety and maintenance of buried public infrastructure. In order to fully automate the condition assessment of buried pipes, it is necessary to develop a robust defect analysis and interpretation system. And presented the development of an automated defect detection system

for sanitary sewer pipelines using digital imaging techniques like contrast enhancement, mathematical morphology and curvature evaluation.

Reis et al. (2005) studied the corrosion damage in steel reinforced mortar using guided waves. Reinforced mortar specimens with seeded defects were used to simulate corrosion damage and monitored using ultrasonic approach. Advantage was taken of the lower frequency (<250 KHz) fundamental flexural propagation mode because of its relatively large displacements at the interface between the reinforcing steel and the surrounding mortar.

Darmawan et al. (2005) states that accelerated pitting corrosion tests have been performed to obtain spatial and temporal maximum pit-depth data for pre-stressing wires. This data is then used to develop probabilistic models of pitting corrosion and strength capacity of 7-wire strands. The probabilistic model of pitting corrosion for strands is then combined with a non-linear Finite Element Analysis and probabilistic models of corrosion initiation and propagation to study the spatial and temporal effects of pitting corrosion on a typical pre-tensioned pre-stressed concrete bridge girder. The limit states considered are flexural strength and serviceability. The spatial time-dependent reliability analysis takes into account the uncertainties and variability related to material properties, dimensions, loads and corrosion parameters as well as the spatial variability of pitting corrosion of pre-stressing strands. Including the spatial variability of pitting corrosion in the reliability analysis increased both the probability of strength and serviceability failure when compared with a mid-span sectional analysis.

Rizzo et al. (2007) discussed a method based on outlier analysis and the wavelet transform for structural damage detection based on guided ultrasonic waves. The basic idea is to de-noise and compress the ultrasonic signals by the discrete wavelet transform and use the relevant wavelet coefficients to construct a unidimensional or multidimensional damage index. The damage index is then fed to an outlier analysis to detect anomalies that are representative of structural defects. By extracting the essential information from the ultrasonic signals, the dimension of the damage index is kept at a minimum, as desirable for continuous structural monitoring. The general framework is applied to the detection of notch-like defects in a seven-wire strand by using built-in magnetostrictive devices for ultrasound transduction. Random noise is digitally added to the

raw ultrasonic measurements to create statistical populations of the baseline (undamaged) conditions and the damaged conditions. This application demonstrates the effectiveness of the multidimensional analysis compared to the unidimensional analysis, while keeping the number of features as low as four.

Garima Vermani et al. (2008) utilized ultrasonic longitudinal guided waves for defect detection in reinforcing steel bars in air and results were analytically verified using ABAQUS software.

Sharma et al. (2010) applied ultrasonic guided waves for corrosion monitoring in RC beams. Corrosion was simulated in the form of debonding and notches on the bars. To assess the suitability of simulation technique, the work was applied to a RC beam undergoing actual corrosion.

Sharma et al. (2010) utilized ultrasonic guided waves for monitoring progression of corrosion in oxide and chloride environments in RC beam specimens.

2.2 ANALYTICAL WORK DONE

In analytical studies the prominent work done is listed here. **Lamb (1904)** made the first investigation of pulse propagation in a semi-infinite solid. **Timoshenko (1921)** developed a theory for beams that accounted for shearing deformation. **Bhalla et al. (2005)** investigated wave propagation approach for NDE using surface bonded piezoceramics.

Washer et al. (2001) applied acoustoelastic concepts to the evaluation of stress levels in pre-stressed rods and strands. The effects of temperature and those of varying boundary conditions on stress measurements were included in this work. Magnetostrictive sensors were developed in for the wave generation and detection. Such sensors lend themselves to wave transduction in tendons, as they consist of electrical-wire coils that can be easily wrapped around the cylindrical member. In magnetostriction, an alternate electrical current in the transmitter coil induces a variation of the magnetic field within the coil that, in turn, produces a change of magnetization within the ferromagnetic test material; the subsequent deformation (Joule's effect) produces a stress wave. The inverse mechanism is used in wave detection; the wave propagating in the ferromagnetic material modulates an existing magnetic field (Villari's effect), thereby exciting a voltage pulse in the receiver coil according to Faraday's law. Magnetostrictive sensors for guided

wave transduction were also employed by **Kwun and Teller (1994)** and by **Kwun et al. (1998)** for stress measurement and defect detection in strands.

Matt (2001) discussed some techniques of non-destructive evaluation and monitoring of post-tensioning tendons like Reflectometrical Impulse Measurement (RIMT) and Acoustic Monitoring and their specific applications and drawbacks.

Au et al. (2003) proposed various design methods for the determination of ultimate tendon stress at flexural failure of pre-stressed concrete beams with unbonded tendons. Two broad categories of deformation-based approaches have been identified, namely those based on the span–depth ratio together with loading type, and those based on the neutral axis depth. These methods are reviewed critically. A new design formula has been proposed in the light of the available experimental data. It is applicable not only to the conventional high-strength steel pre-stressing tendons, but also to those made of other materials such as fibre-reinforced polymer.

Francesco Lanza di Scalea et al. (2003) described that health monitoring of steel strands is the subject of much research in the nondestructive evaluation and civil engineering communities. And deals with a guided stress wave method for stress monitoring and defect detection in seven-wire strands. A simplified acoustoelastic formulation of the Pochhammer-Chree vibrations in cylindrical waveguides is derived in the framework of the partial wave representation for guided waves. Magnetostrictive transducers are used to excite and detect the waves in the experiments. Results from acoustoelastic measurements on single wires and on strands are presented, showing the feasibility of the method for stress measurement, although an anomalous behavior of the strands at low stress levels remains the subject of current investigation. Improvements to the inherently low sensitivity of acoustoelastic stress measurements are suggested by adding the effect of strand elongation. The role of the strand anchorages is also examined in the context of wave attenuation. Finally, the suitability of the guided wave method for the detection of indentations and broken wires in the strands is demonstrated, including the possibility of inspecting the critical anchored regions.

Gharighoran et al. (2008) described that a mode-based damage identification technique is proposed to predict damage location and severity in the post-tensioned concrete beams for the first time. Damage-induced changes in modal characteristics can be detected using experimental modal analysis. Based on changes in natural frequency, mode shapes, and damping ratios, a methodology for detecting damage location and severity is presented. The damage was induced by application of point load at half span location on the reinforced and post-tensioned concrete beams. The load was gradually increased to obtain different crack patterns to be used in simulation of damage scenarios. Experimental modal analysis was performed on the undamaged and damaged beams. The natural frequency and mode shapes were used to determine the location of damage. The approach is developed at an element level with a conventional finite element (FE) model by Ritz method, which is called Ritz damage detection method (RDDM). The mathematical model for both damped and undamped damaged structures have been established through the eigenvalue equations. The singular value decomposition (SVD) technique is used for determination of damage or sound index. These indexes are sensitive to the change of dynamic characteristics due to damages. This approach is applied to five simply supported post-tensioned concrete beams. The numerical results show that the exact location and severity of damage for different simulated damage scenarios could be efficiency found by the present methodology.

Kim et al. (2009) described that a hybrid health monitoring system using sequential vibration-impedance approaches is newly proposed to detect two damage types, which are tendon damage and girder damage, in PSC girder bridges. It mainly consists of three sequential steps: global damage warning, damage classification, and damage estimation. In Step 1, global occurrence of damage is warned by monitoring changes in acceleration features. In Step 2, damage types are classified into either tendon damage or girder damage by recognizing patterns of vibration and impedance features. In Step 3, the location and the extent of damage are estimated by using a mode shape-based method and a frequency-based method. The feasibility of the proposed system is evaluated on a laboratory-scaled PSC girder model for which acceleration responses and electro-mechanical impedances were measured for several damage scenarios of tendon damage and girder damage.

2.3 CLOSING REMARKS

This chapter gives a brief review of state of art for damage monitoring using ultrasonic guided waves. Some recent works establish the fact that ultrasonic guided waves can be used for damage monitoring of reinforcing bars in concrete **[Sharma et al. (2010)]**. It is proposed to use the guided waves for damage detection in PSC tendons in concrete in this research work.

CHAPTER 3

ULTRASONIC INVESTIGATIONS OF TENDONS WITH SIMULATED CORROSION DAMAGES

3.1 GENERAL

The main effects of corrosion degradation result from rust formation at the outer surface of the pre-stressing steel with the corresponding steel cross-sectional loss. Rust product is widely accepted as being more voluminous than steel, with reports ranging from twice to six times the volume. **[Broomfield et al. (2002)]** an increase in rust product accumulation at the interface, results in eventual cracking which causes a loss of bond between the tendon and concrete which is called as delamination. Cracking of the surrounding concrete caused by the continuing pressure buildup from corrosion product is the main form of degradation to the surrounding concrete. Cracking, spalling, and rust staining are usually the earliest indications of corrosion in the concrete. Cracking usually occurs at small percentages of loss of steel mass, usually around a rust thickness of 0.1 to 0.2 mm.

In the laboratory, uniform corrosion is relatively easier to achieve than localized corrosion. However, uniform corrosion is virtually nonexistent in a realistic situation. Instead, pits (crevices) of corrosion are generally found scattered along the bars or tendons in concrete.

Pitting of the steel causes reflections of the wave form and mode conversions leading to the overall attenuation of the signal strength of the transmitted mode. In an infinite isotropic solid medium only two types of independent wave propagation exist, i.e., compressional and shear waves. Both waves propagate with constant velocities and are nondispersive.

In this chapter, corrosion in tendons is simulated in the form of area reduction (pitting) and debonding (delamination) from the surrounding concrete. The next section discusses the experimental details of simulated corrosion studies.

3.2 EXPERIMENTAL SET UP

The ultrasonic testing system consisting of a pulser /receiver, transducers, and display devices was used **(Fig.3.1)**. Driven by the pulser, the compressional transducer generates ultrasonic pulse that propagates through the bar in the form of longitudinal waves. When there is an interface such as a crack, void or flaw in the wave path, part of the energy is reflected back from the interface and received by the same transmitting transducer. The reflected energy is converted into an electrical signal which is processed in a computer and digitized for display. From the display, the time of flight between the excitation and reflected pulse is measured. Knowing the group velocity of the excited longitudinal wave mode, the location of the defect can be calculated as follows:

D= Vt/2..…… (3.1)

Where, D = Distance of defect from transducer end, V = Group Velocity of excited mode and t = Time of Flight

This method of testing is called pulse echo method.

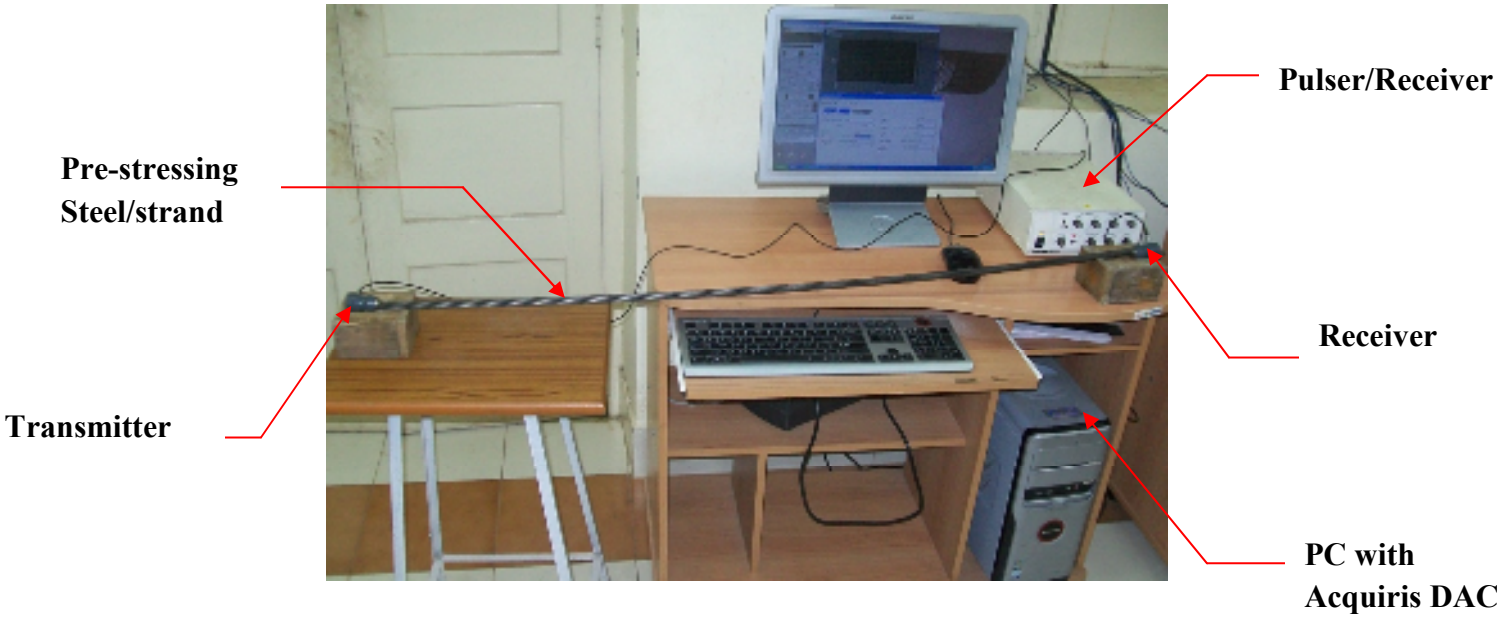

Fig.3.1 Experimental Set up

Conventional techniques of Pulse echo and Pulse transmission method were used for characterizing the damage. To find the location of crack, pulse echo method is used and to find the extent of damage both pulse echo and pulse transmission are used. A single contact transducer is used to generate and receive wave signatures in the pulse-echo method. Two contact transducers are used for sending and receiving the waveforms in pulse transmission method. Transducers ACCUSCAN "S" series having a longer wave form duration and a relatively narrow frequency bandwidth with centre frequency of 1 MHz is used for the 12.7 mm strands. A computer with an ACQUIRIS digitizer card was used to capture the received signal and its processing. The transducer is mounted in a holder and attached to the specimens using an industrial coupling gel **(Fig.3.1)**. The excitation signal consisted of a compressive spike pulse with duration ranging from 10-70 ns.

3.2.1 Equipments details

- ***Transducers***

A contact transducer is a single element longitudinal wave transducer intended for use in direct contact with a test piece. It can be used in straight beam flaw detection and thickness gauging, detection and sizing of delamination, material characterization and sound velocity measurements, inspection of plates, billets, bars, forgings castings, extrusions, and a wide variety of other metallic and non-metallic components. ACCUSCAN "S" series have longer wave form duration and a relatively narrow frequency bandwidth. S 12 HB 1 (KARL DEUTSCH) Standard contact transducer of 1 MHz frequency and 12 mm diameter was used.

- ***JSR ultrasonics DPR 300 pulser/ receiver system***

DPR300 pulser produces a high voltage electrical excitation pulse and applies this pulse to the instrument's T/R connector. An ultrasonic transducer connected to the T/R connector via a length of 50 Ω coaxial cable is then employed to convert the electrical energy of the excitation pulse into an ultrasonic pulse that is propagated into a test material or medium.

With the DPR300 configured for pulse-echo mode operation, acoustic echoes reflected from interfaces or defects within the test material are converted by the transducer into electrical signals that are presented to the T/R connector of the DPR300. The low-noise DPR300 receiver amplifies these electrical signals, and the signals then pass through adjustable high pass and low pass filters. The DPR300 receiver gain is adjustable between -13 dB and 66 dB, and there are six high pass and six low pass filter settings for band-limiting the receiver frequency response. The amplified and filtered signals are available on the instrument's Receiver Output connector.

The DPR300 may also be used in transmission mode operation wherein a separate receiving transducer is used to detect acoustic pulses that have propagated through a test material or medium.

PRF oscillator & pulser trigger control: The internal PRF oscillator generates repetitive trigger pulses for the pulser subsystem under the control of the PRF control. Pulser Trigger control selects between the internal PRF oscillator or an external source applied to the Trig/Sync connector as trigger sources for the DPR 300 Pulser.

Pulser (impedance/energy/damping): The pulser generates an excitation pulse upon receiving a trigger event from a selected source. There are four energy and two impedance values, and the single Energy and impedance control adjusts the pulse energy and the pulser impedance.

Receiver amplifier: It controls the amplification or attenuation of signals processed by the DPR300 receiver. The receiver gain can be varied from -13dB to 66 dB.

Low pass and high pass filters: Low filters are available for reducing the bandwidth of the DPR300 receiver. High Pass filters are available for eliminating undesirable low frequency energy from the DPR300 receiver signal. High pass filtering can be used as a means of providing faster receiver recovery from strong signals such as the excitation pulse or strong interface echoes.

Pulser	
Pulse Type	Negative Spike Pulse
High Voltage Supply	100V to 475V
Initial Transition (Fall Time)	<5 ns (10-90%) typical for 475V pulsers
Pulse Amplitude	-475V peak. Amplitude depends on Energy, Impedance, Damping control settings, and pulser type
Pulse Energy	1.55 µJoules minimum, 304 µJoules maximum for 475V pulsers. Dependent upon energy and voltage setting
Pulse Duration	Typically 10-70 ns FWHM for 50 Ω load. Function of the Energy, Impedance, and Damping controls
Damping	16 Damping values: 331, 198, 142, 110, 92, 77, 67, 59, 52, 47, 43, 39, 37, 34, 32, and 30 Ω
Mode	Pulse-echo or through transmission
Through Mode Isolation	Typically 80 dB at 10 MHz
Pulser Repetion rate	Internal: 100 Hz -5 kHz for 475V pulsers. External: 0-5 kHz for 475V pulsers.
Sync Output	Maximum +5 V, tr <30 ns, tw=50 ns.min. TTL and CMOS compatible. Minimum value of load impedance is 50 Ω
Pulser Trigger Source	Selectable by computer between internal oscillator and external source
External Trigger Input	3 - 5 V positive going pulse. Triggering will occur synchronously with leading edge of trigger signal. TTL and CMOS compatible
Receiver	

Gain	-13 to 66 dB in 1 dB steps controlled by the host computer
Phase	0° (noninverting)
Input Impedance	500 Ω (through transmission)
Bandwidth	.001-35 MHz (-3 dB) or .001-50 MHz
High Pass Filter	DC,1,2.5,5,7.5 and 12.5 MHz
Low Pass Filter	3,7.5,10,15,22.5 (35 MHz BW) or 5,10,15,22.5,35 (50 MHz BW)
Receiver Noise	Typically 49 μV pk-pk input referred (measured at 60dB,35 MHz bandwidth)
Output Impedance	50 Ω
Output Voltage	± 0.5 V into 50 Ω

- ***Dual-channel high-resolution waveform digitizer***

Model DC438 Dual-channel, 12-bit, 100 MHz, 200 MS/s, 4 M point acquisition memory card was used to capture the waveform. Waveforms are transferred directly into the digitizer large acquisition memories so that complex signals can be stored over very long time periods. Large memories are essential for maintaining fast sampling rates and therefore timing resolution.

Model DC438	
Bandwidth (-3 dB)	DC to 100 MHz
Full Scale Range (FSR)	250 mV, 500 mV, 1 V, 2 V, 5 V and 10 V
Impedance	50 Ω ± 1% @ DC
Connector	BNC, gold-plated
Channels	Two
Coupling	DC

Maximum Input Voltage	±10 V DC (2 W) or 10 V RMS at 50 Ω
Bandwidth Limit Filter	35 MHz 2-pole Bessel filter (DC438)
Minimum Amplitude	1 V pk-pk
Impedance	50 Ω

3.3 SPECIMEN DETAILS

Corrosion is simulated in the form of pitting causing area reduction and delamination resulting in debonding from surrounding cover. First testing is carried in P/E and P/T modes in strands/tendons in air simulating pitting. Then the testing is extended to tendons with simulating delamination and pitting effects in concrete/mortar.

3.3.1 Testing in air

To simulate corrosion damage, pre-stressing steel strands of 12.7 mm external diameter and 1.2 m length is used for experiments. The damage is introduced in the form of notches (area reduction) at two different locations, at middle (L/2) and at one-third (L/3) of the strand where L is the length of the strand. For a particular location with 0%, 20%, 40% and 60% area reduction is prepared **(Fig.3.2)**. Two samples of each specimen are tested to examine the repeatability and precision of results. These four sets of specimen are first ultrasonically tested in air. Pulse echo and pulse transmission method are used for characterizing the damage. To find the location of crack, pulse echo method is used. In pulse transmission method, two probes were used one as an actuator for sending the waves at one end and another as a receiver for receiving the waves at the other end of the strand.

3.3.2 Testing in concrete/mortar

The study was extended to another same set of specimens which are cast in concrete. In concrete, damages in the form of notches (area reduction) and delaminations are introduced at a particular location of the strand is simulated as area reduction of 0%, 20%, 40% and 60% diameter reduction at different damage locations (L/2 & L/3) **(Fig.3.2)**. Delamination is simulated by

wrapping a double sided tape to 25%, 50%, 75% and 100% length of the strands before placing it in concrete **(Fig.3.3 (a))**. The diameter of the strand is 12.7 mm and the length of the strand is 1.2 m was placed at the centre of cross section of the beam at the time of casting. The strand projected out by 250 mm on each side of the beam and the dimensions of the beam is 150 x 150 x 700 mm **(Fig.3.3 (a & b))**. Concrete with proportions of cement, sand and stone aggregates as 1:1.5:3 is used for casting. The water cement ratio is kept as 0.5. Two samples of each specimen were tested to examine the repeatability and precision of results. These are ultrasonically tested in concrete. Both P/E and P/T testing is done. In pulse-transmission method of testing an ultrasonic transmitter introduces wave from one end of the bar and a receiver is placed at the opposite end to record the transmitted pulse. By measuring the relative change of the amplitudes of the input and the received signals, the relative severity of the flaw is assessed. The results were reported in the form of voltage-time curve (V-T). **Fig.3.4** defines overall test matrix for simulated corrosion studies.

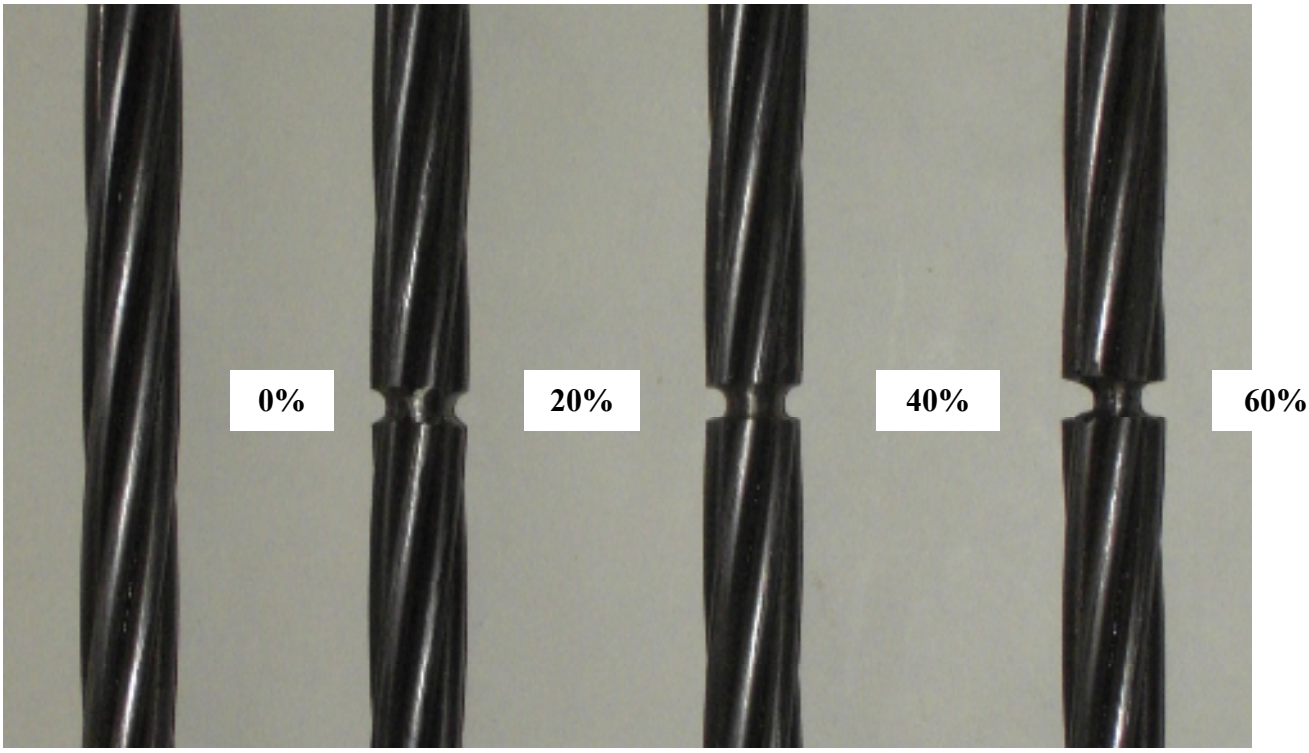

Fig.3.2 Strands with 0%, 20%, 40% and 60% diameter reduction at a particular location

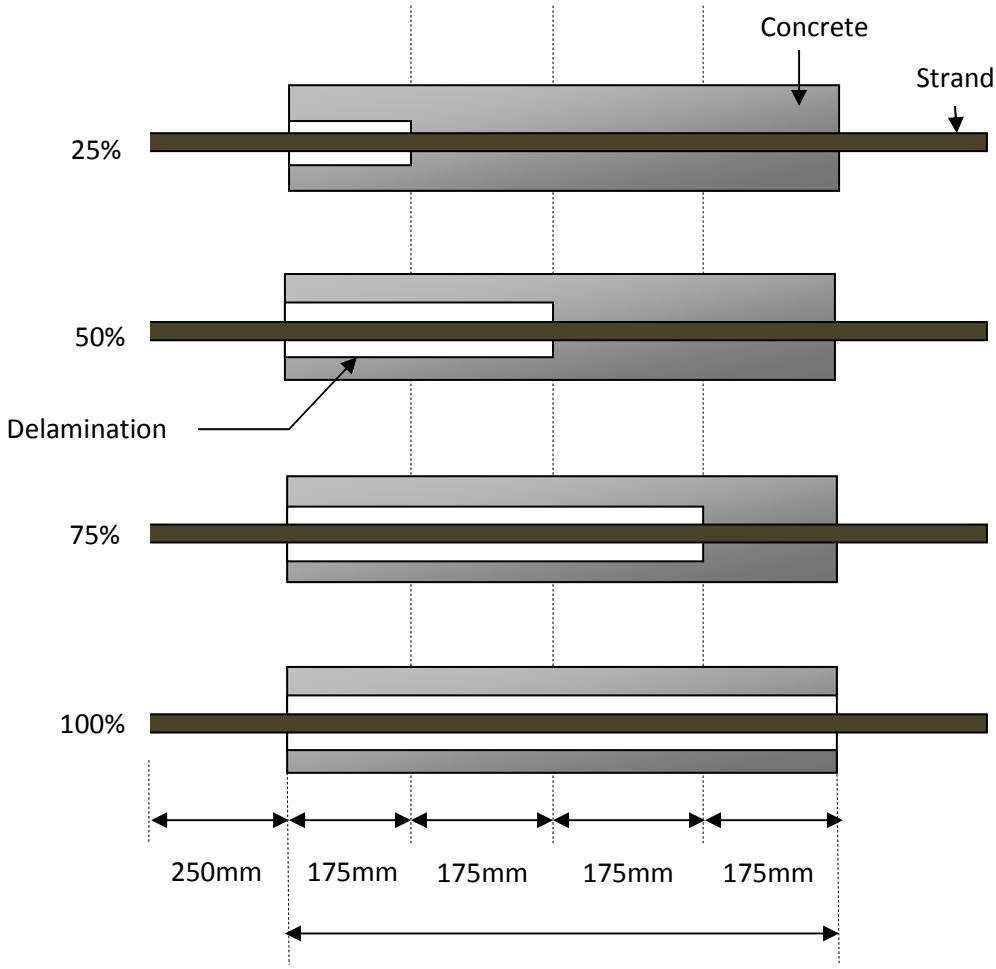

Fig.3.3 (a) Specimens inspected

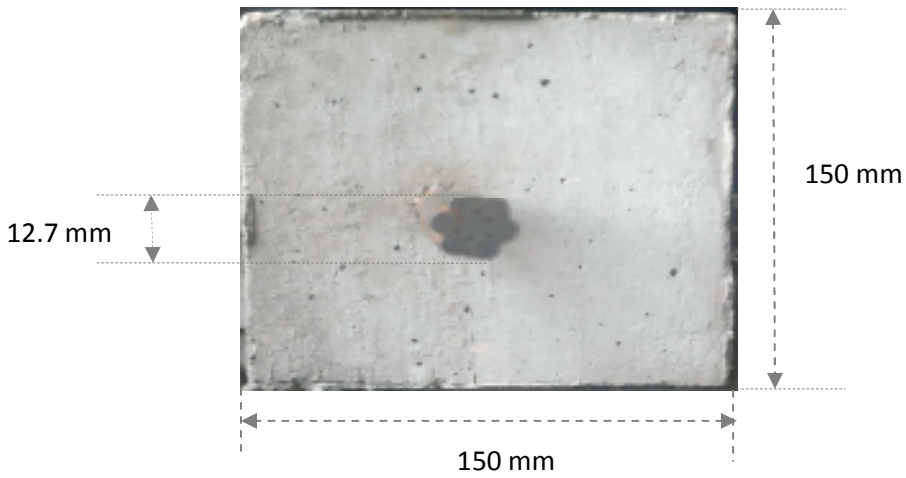

Fig.3.3 (b) Cross-sections of concrete beam with pre-stressing tendon

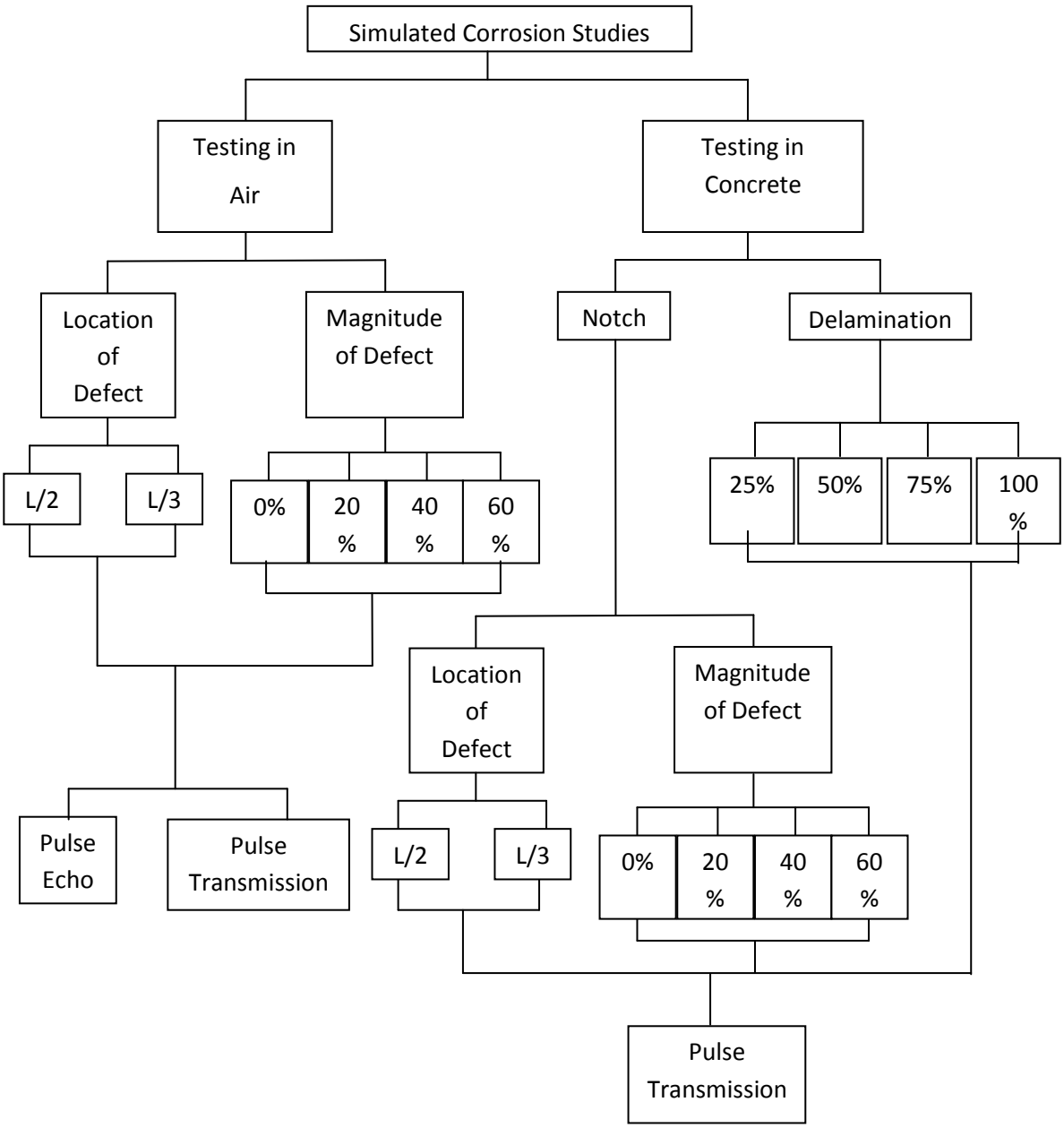

Fig.3.4 Test matrix for simulated corrosion studies

3.4 SELECTION OF EXCITATION MODE AND FREQUENCY

In an infinite bulk of a perfectly elastic material, ultrasonic waves travel as bulk waves in the form of compressional and shear waves. Both the waves propagate with constant velocities. They are non-dispersive and decay in amplitude because of the spread of the wave front. However, in a finite perfectly elastic media like a pre-stressing strand, the ultrasonic wave is reflected from its boundaries, and the energy is contained within the strand as a guided wave. The complex effect of the strand boundaries results in dispersion of the wave and generates different modes that have predictable properties such as mode shapes and frequencies. They can be calculated by solution of the wave propagation equation. The solution of the wave propagation equation yields a number propagating modes. The velocity-frequency relationships of guided waves are displayed as dispersion curves. A global matrix method is employed for solution of wave propagation equation using optimization techniques (Lowe, 1995). The method was then developed into a standard software Disperse (Lowe, 1995; Pavlakovic and Cawley, 2000).

In the present work, pre-stressing strands of 12.7 mm diameters are chosen for the study. Longitudinal waves having no angular displacements and exhibiting only radial and axial displacements were chosen. Non-axi-symmetric flexural waves exhibit high attenuation and hence were not considered. Also it is easier to invoke a strong longitudinal wave. They are produced in the strands by keeping compressional transducers parallel to the guiding configuration at the two ends of the bars. The different longitudinal modes are excited by varying the excitation frequencies. The selection of frequencies is done based on the phase velocity dispersion curves. They are validated by experimentally confirming the signal fidelity.

For strand testing in air, mode having best signal output and with velocity close to bulk longitudinal velocity is chosen for testing. L (0, 11) at 1MHz mode **(Fig.3.5)** is chosen for ultrasonic testing.

For strand testing in concrete, high frequency low loss modes having high energy velocity and minimum attenuation is chosen. L (0, 7) at 1MHz is such a mode chosen for ultrasonic investigation **(Fig.3.6)**.

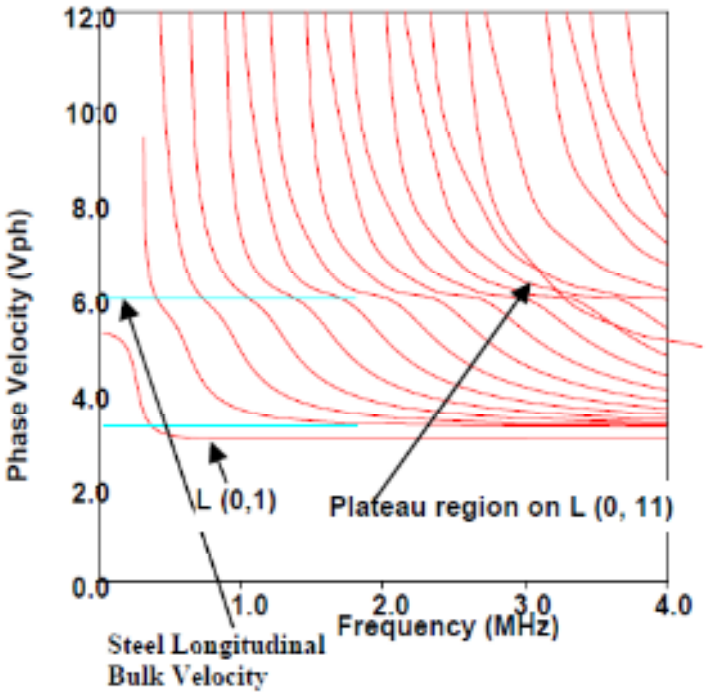

(a) Phase Velocity Dispersion Curve

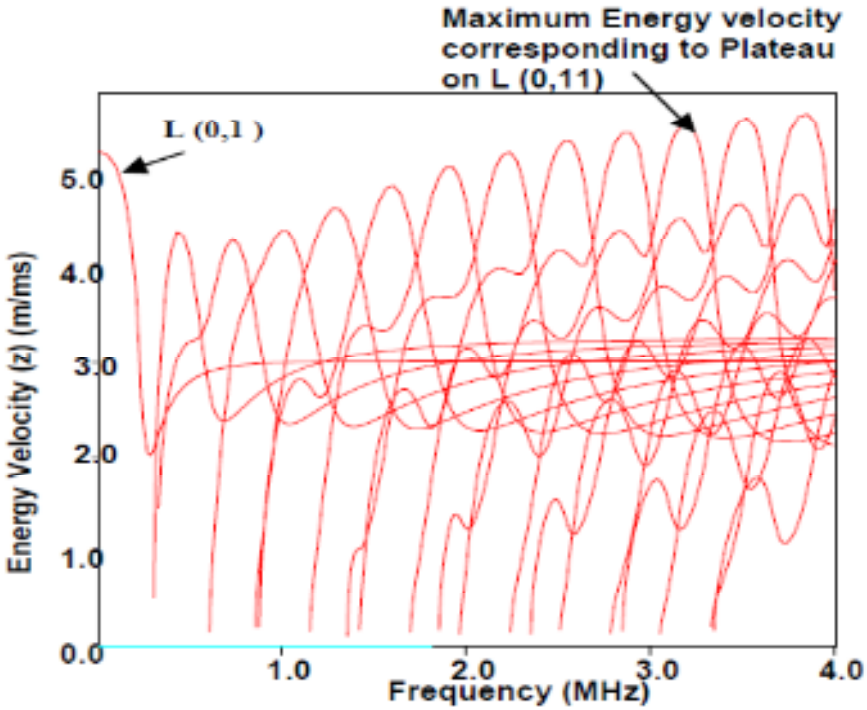

(b) Energy Velocity Dispersion Curve

Fig.3.5 Dispersion Curve for L (0, 11) mode

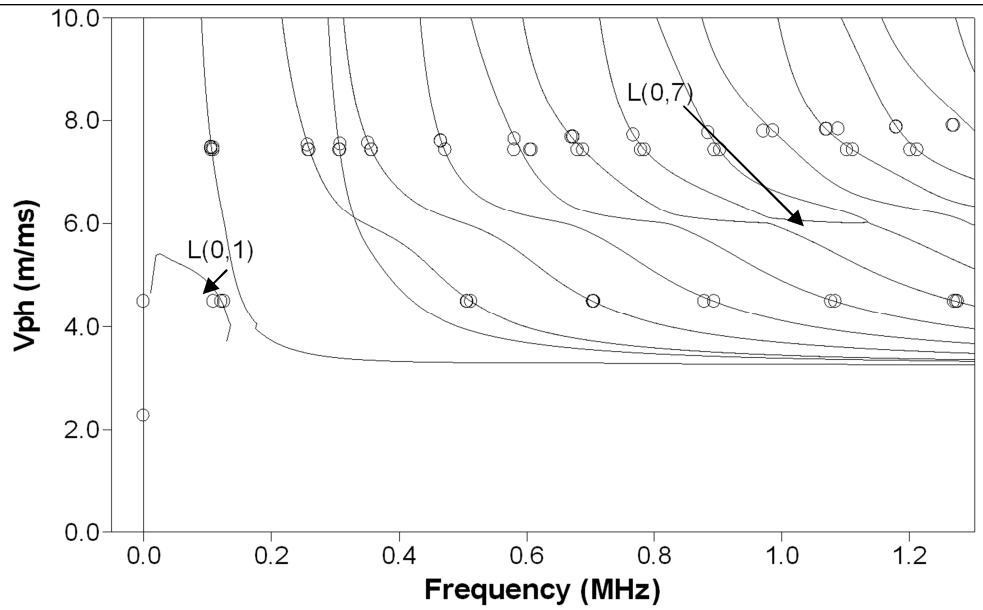

(a) Phase velocity Vs Frequency

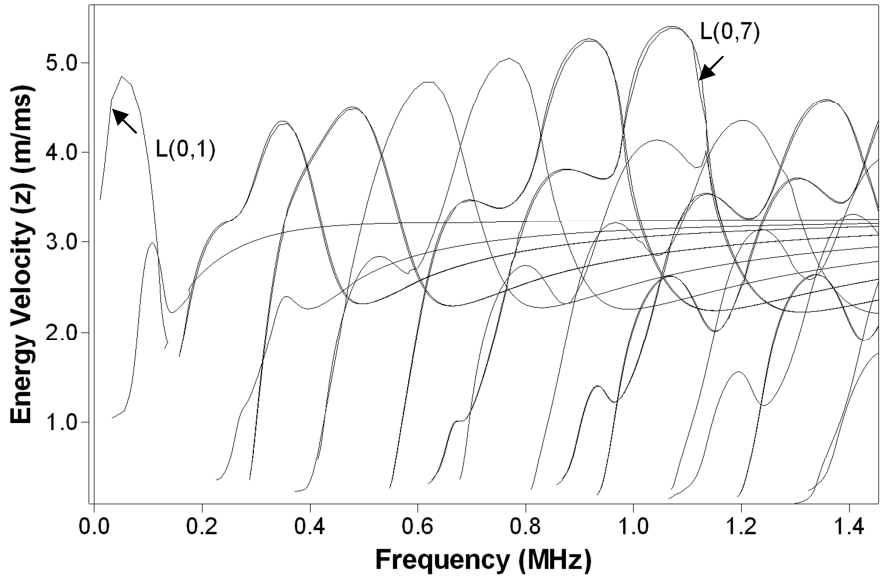

(b) Energy Velocity Vs Frequency

Fig.3.6 Dispersion Curve for L (0, 7) mode

3.5 EXPERIMENTAL RESULTS AND DISCUSSIONS

3.5.1 Testing in air

Four sets of specimens were prepared of 0%, 20%, 40% and 60% area reduction at two different locations, one at L/2 (centre) of the strand of length 1.2 m and other at L/3 (one-third) of the strand. Two samples of each specimen were tested to see the repeatability and precision of the data collected. Testing is done in both P/E and P/T modes. Time of flight of the peak received after reflection from notch will locate the notch. Relative changes in magnitudes of the reflected and transmitted peaks will relate to the magnitude of damage.

3.5.1.1 Pulse echo testing

In the pulse echo method, two reflections are obtained –one from the notch (NE) and another from the back wall (BWE). In a healthy specimen, the peak obtained is only the BWE. **(Fig. 3.7 (a))** shows a typical healthy strand signature. In a notched specimen, the 1^{st} peak is NE and the 2^{nd} peak is the BWE. **(Fig. 3.7 (b-d))** shows the typical pulse echo signatures for notched strands with different extent of notches.

Appearance of a notch echo (NE) indicates the presence of defect in the bar. By knowing the time of flight of NE, location of damage can be computed from **Equation (3.1)**. Comparing the peak-peak voltage amplitudes of NE's and BWE's with reference to the input pulse, extent of damage can also be judged in **(Fig.3.8 (a & b))**. Comparisons of relative amplitudes of the reflected and transmitted pulses with reference to input pulse indicate about the extent of damage. Testing is carried out by keeping the settings of the P-R system as shown in **Table 3.1**.

Table 3.1 Testing of tendons in air (P/E)

JSR DPR 300 Pulser/Receiver settings	
Receiver	
Bandwidth	35
Gain [-12 dB-67 dB]	45 dB
High Pass Filter [Out-12.5 MHz]	Out
Low Pass Filter [3 MHz-35 MHz]	7.5 MHz
Pulser	
Damping [331 ohms-30 ohms]	30 Ohms
Energy [1-4]	4
PRF [100 Hz-5 KHz]	100 Hz
Voltage [100V-400V]	475 V
Impedance [Low-High]	High

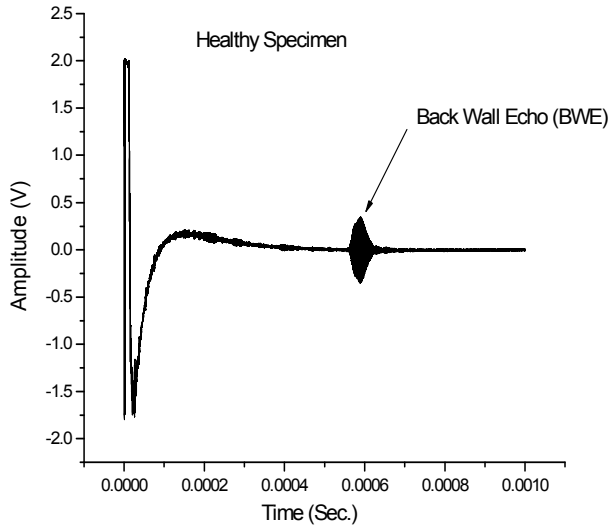

(a) 0%

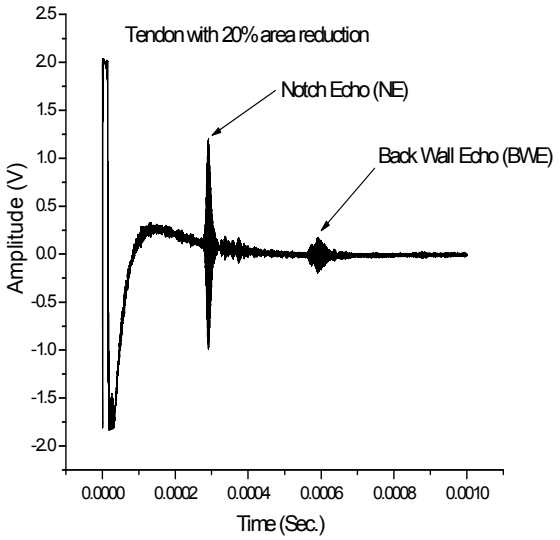

(b) 20%

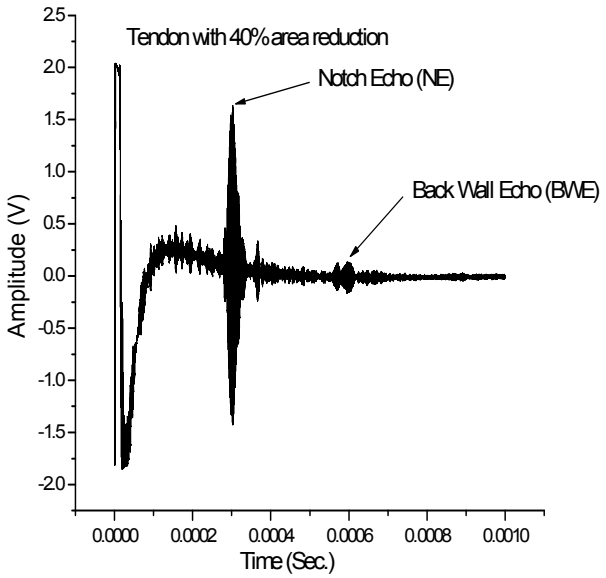

(c) 40%

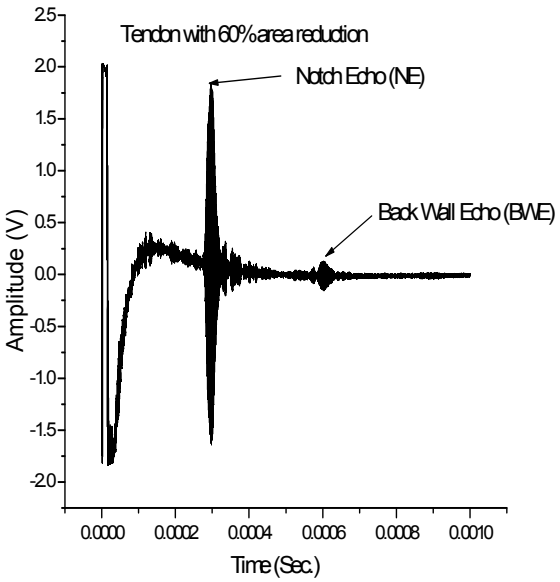

(d) 60%

Fig.3.7 (a-d): Pulse Echo signatures (Notch at L/2)

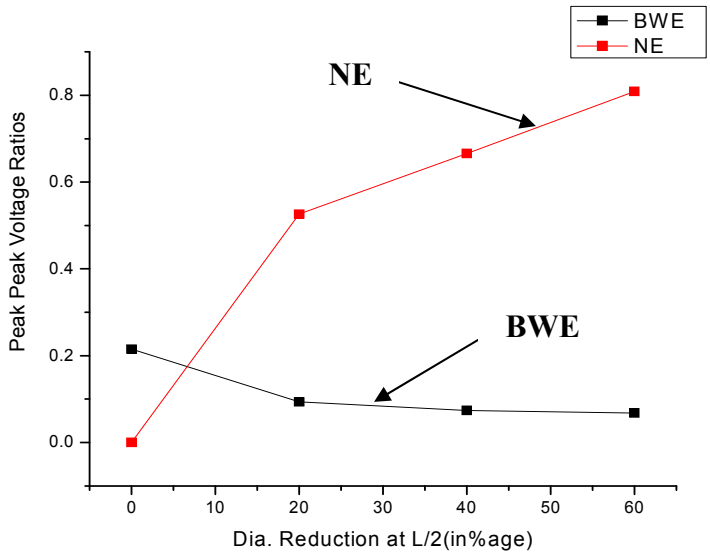

Fig.3.8 (a & b): Peak to peak voltage ratio trends of NE & BWE (Notch at L/2)

Observations in pulse echo testing

- It may be noted that it is fairly simple to identify a defect in the pulse echo technique. Appearance of a peak between the initial pulse and BWE in pulse echo indicates the presence of damage or defect in the strand specimen **(Fig.3.7)**.
- Once the damage is detected, its location can be ascertained.
- After ascertaining the presence and location of damage, the next step is to evaluate its extent. The magnitude of damage can be directly related to the magnitude of the peak received after reflection from the notch (NE) as well as BWE. The amplitude of NE increases and that of BWE reduces with the increase in the notch dimensions **(Fig.3.8)**. By comparing the NE and BWE amplitude with reference to input pulse a qualitative idea about the extent of damage can be made. As the depth of the notch increases more energy is reflected back from it and less of it travels to the back wall. Hence, pulse echo can be effectively used for damage detection in strands. It not only indicates the presence of damage but also gives its exact location and an idea about its extent.

3.5.1.2 Pulse transmission testing

In pulse transmission method, signatures are obtained by placing the emitting and receiving transducers at opposite ends of the strands. In a healthy specimen, peaks are obtained after travelling 'L' and '3L' distances as transmitted pulses (P/T). In the notched specimens a peak appears between the two peaks. This is due to reflection from the notch. **(Fig.3.9 (a-d))** shows the signature of the healthy and notched strands. The notch is at L/2. Therefore, the peak due to the notch should appear in the middle of L and 3L peaks of the healthy strand.

The peak was not clearly observed at 20% notch. However, the peak rose considerably with increasing depth of the notch.

When one compares these results with pulse echo results, the NE was very clearly visible at the lowest depth of notch. Hence, pulse echo is a better indicator of the presence of the notch rather than pulse transmission technique. Testing is carried out by keeping the settings of the P-R system as shown in **Table 3.2**.

Table 3.2 Testing of tendons in air (P/T)

JSR DPR 300 Pulser/Receiver settings	
Receiver	
Bandwidth	35
Gain [-12 dB-67 dB]	40 dB
High Pass Filter [Out-12.5 MHz]	Out
Low Pass Filter [3 MHz-35 MHz]	7.5 MHz
Pulser	
Damping [331 ohms-30 ohms]	30 Ohms
Energy [1-4]	4
PRF [100 Hz-5 KHz]	100 Hz
Voltage [100V-400V]	475 V
Impedance [Low-High]	High

Observations in pulse transmission testing

- In pulse transmission arrival time remains unchanged due to varying location of notch. Thus, it is not feasible to ascertain the location of the damage using pulse transmission technique.
- But pulse echo is a preferred method for damage location since NE is more discernible and it directly gives the location. The extent of damage in strand can be ascertained by observing the peak to peak voltage trends of P/T. As the % of damage increases from 0% to 60%, the magnitude of the transmitted peak reduces continuously **(Fig.3.10)**. This is because as the notch dimensions increases, more energy is reflected back and less of it travels through the strand to reach at the other end. Hence, relative signal attenuation of P/T can relate to the extent of the damage in the strand.
- However, the signal attenuation was not linear with the depth of notch. P/T values dropped very gradually with increase in notch dimensions. This is attributed to the parabolic input pressure profile with the peak at its centre generated by the transducer. Thus, most of the energy is able to pass through the core portion of the strand even though its periphery is notched.

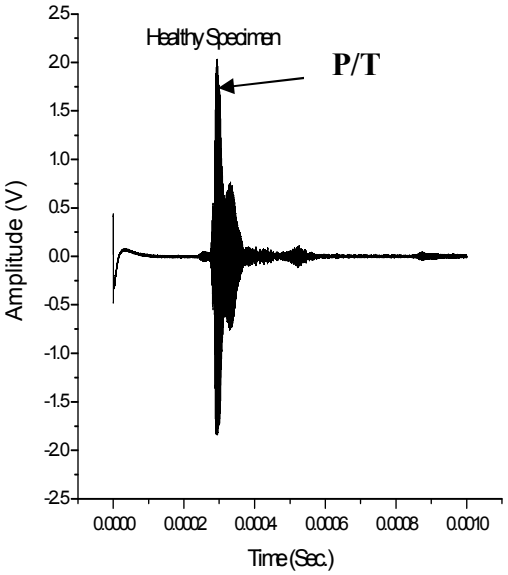

(a) 0%

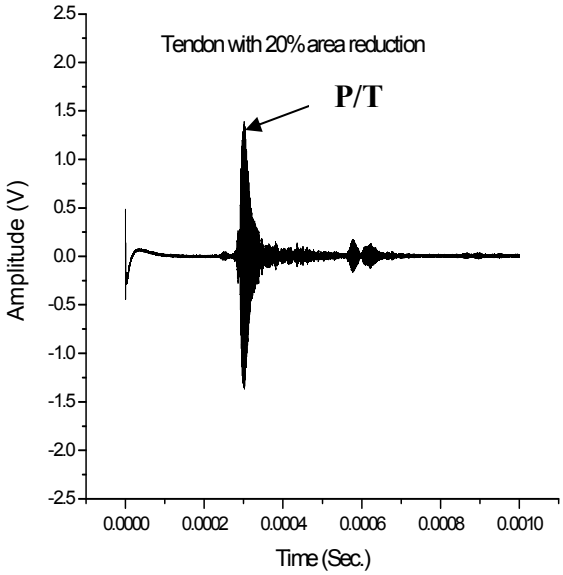

(b) 20%

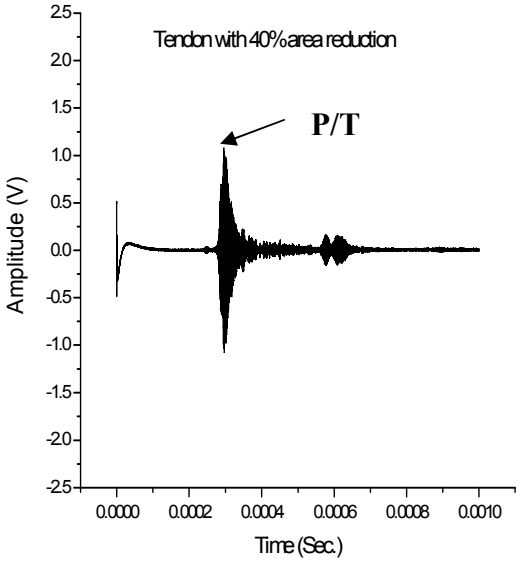

(c) 40%

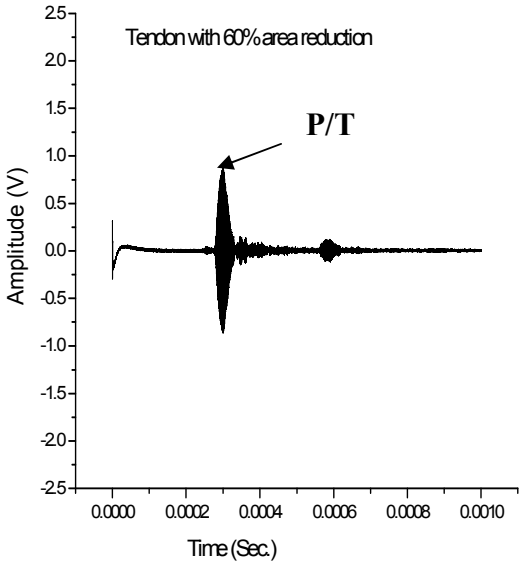

(d) 60%

Fig.3.9 (a-d): Pulse Transmission signatures (Notch at L/2)

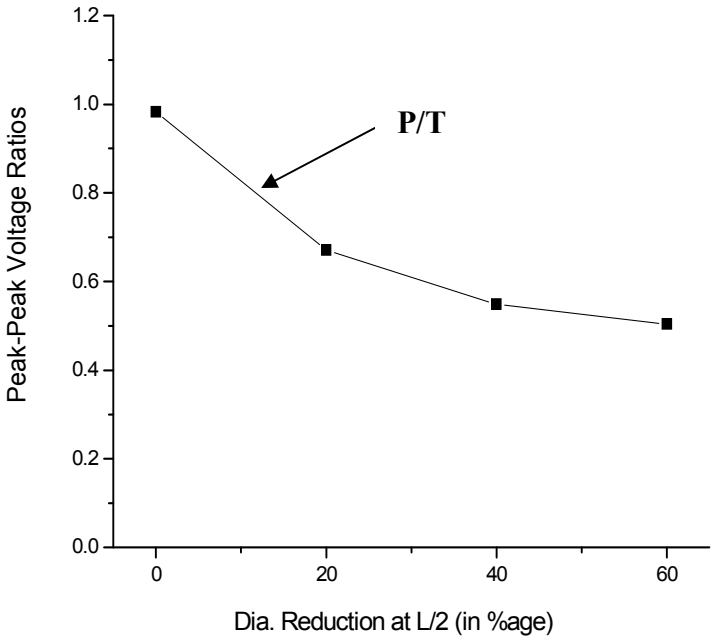

Fig.3.10: Peak to peak voltage ratio trends of P/T (Notch at L/2)

3.5.1.3 Effect of variation in damage location

As the damage location is varied from L/2 to L/3 in the strand, the results followed same trends for peak to peak voltage amplitudes in Pulse Echo and Pulse Transmission testing as for strand with notch at centre **(Fig.3.11)** and **(Fig.3.12)**. Location of damage can be ascertained from the time of flight of NE from pulse echo signatures. Extent of damage can be judged from the peak to peak voltage amplitude ratios of the P/T in pulse transmission. Also an idea can be obtained about extent of damage by observing peak to peak voltage amplitude ratios of NE and BWE in pulse echo testing.

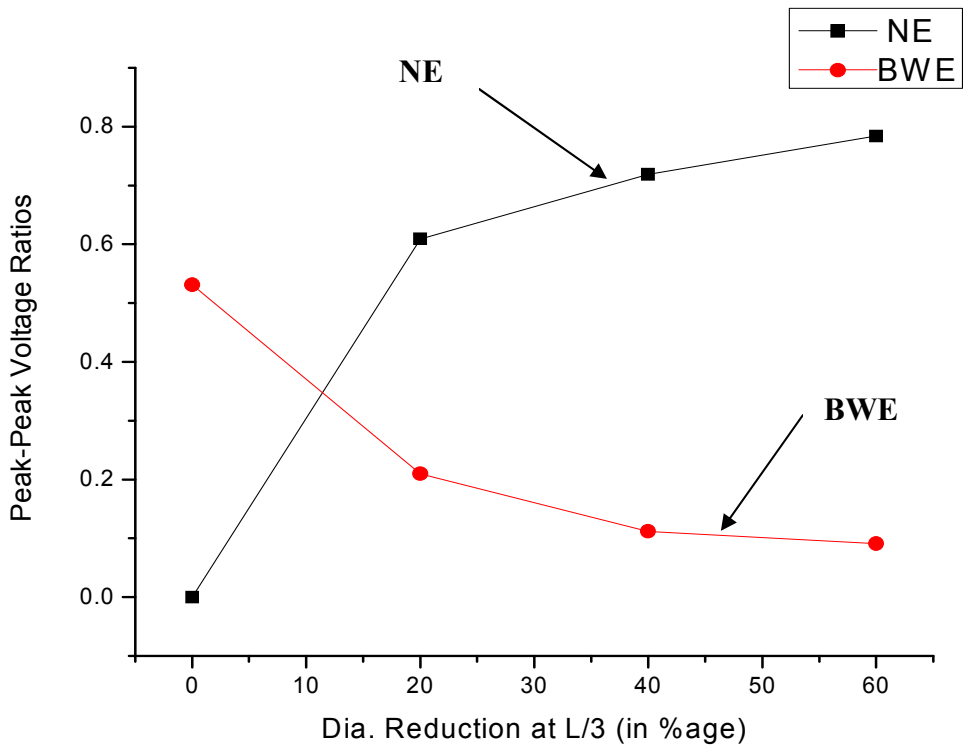

Fig.3.11: Peak to peak voltage ratio trends of NE & BWE (Notch at L/3)

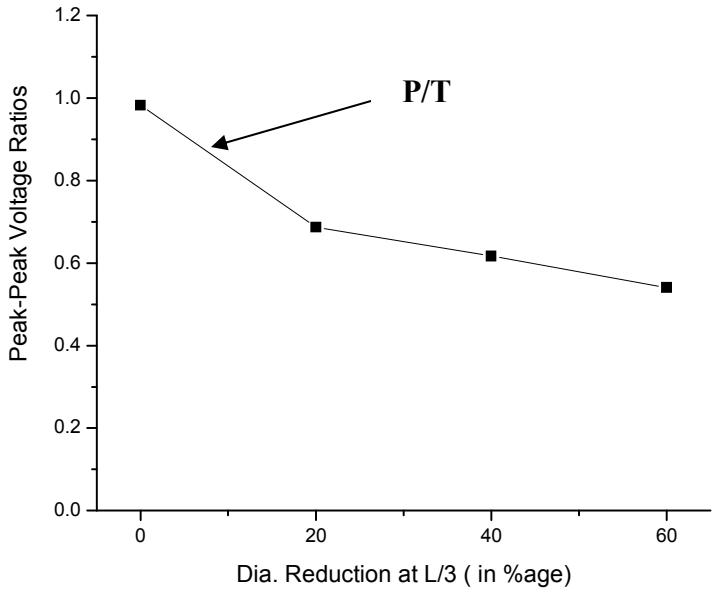

Fig.3.12: Peak to peak voltage ratio trends of P/T (Notch at L/3)

3.5.2 Testing of tendons embedded in concrete

Tendons with damages in the form of notches (area reduction) and delaminations were introduced at a particular location of the strand with 0%, 20%, 40% and 60% diameter reduction at different damage locations (L/2 & L/3) and delaminated with 25%, 50%, 75% and 100% length of the strands are cast in concrete. Two samples of each specimen were tested to see the repeatability and precision of the data collected. Testing is carried out only in pulse transmission mode. This is because of the presence of attenuating concrete, leakage of energy takes place and hence no peaks are obtained in P/E. Also because of layer surface area of tendons leakage further increases.

3.5.2.1 Simulated notch damage

Damage in the form of notch is introduced in strand and then embedded in concrete. The results followed same trends for peak to peak voltage amplitudes in pulse transmission testing as for strand in testing air corrosion as discussed earlier. **(Fig.3.13 (a-d) & 3.14)** shows signatures and peak to peak voltage ratios trends of P/T with 0% (healthy), 20%, 40% and 60% area reduction at L/2 location. **Table 3.3** shows the instrument settings for P/T excitation in strands in concrete (Notch at L/2).

The extent of damage can be ascertained by observing the peak to peak voltage trends of P/T. As the % of damage increases from 0% to 60%, the magnitude of the transmitted peak reduces continuously **(Fig.3.14)**. This is because as the notch dimensions increases, more energy is reflected back and less of it travels through the strand to reach at the other end. Hence, relative signal attenuation of P/T can relate to the extent of the damage in the strand. However, the signal attenuation is not linear with the depth of notch. P/T values drops very gradually with increase in notch dimensions. For tendons testing in P/E, it is required to increase the input energy of the P/R system so that NE and BWE can be obtained.

Table 3.3 P/T testing in strands in concrete (Notch at L/2)

JSR DPR 300 Pulser/Receiver settings	
Receiver	
Bandwidth	35
Gain [-12 dB-67 dB]	65 dB
High Pass Filter [Out-12.5 MHz]	Out
Low Pass Filter [3 MHz-35 MHz]	7.5 MHz
Pulser	
Damping [331 ohms-30 ohms]	47 Ohms
Energy [1-4]	4
PRF [100 Hz-5 KHz]	100 Hz
Voltage [100V-400V]	475 V
Impedance [Low-High]	High

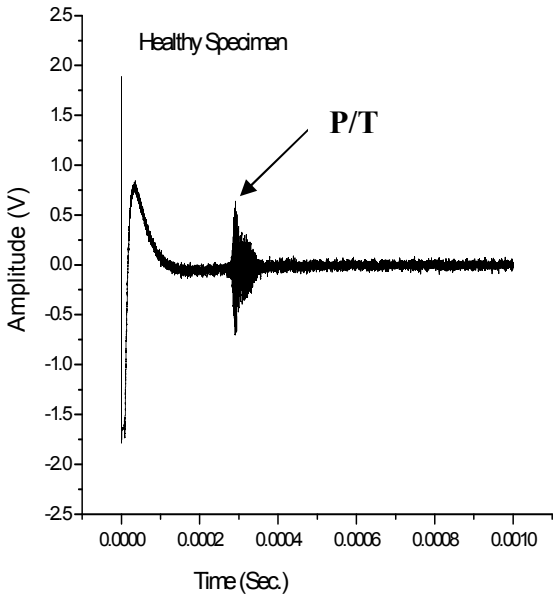

(a) 0%

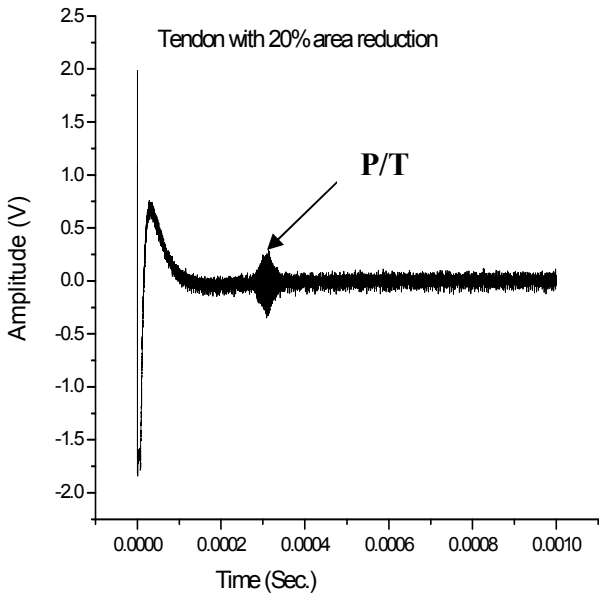

(b) 20%

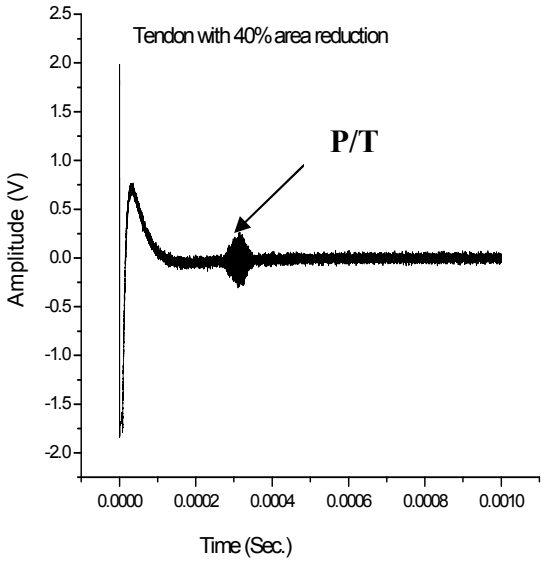

(c) 40%

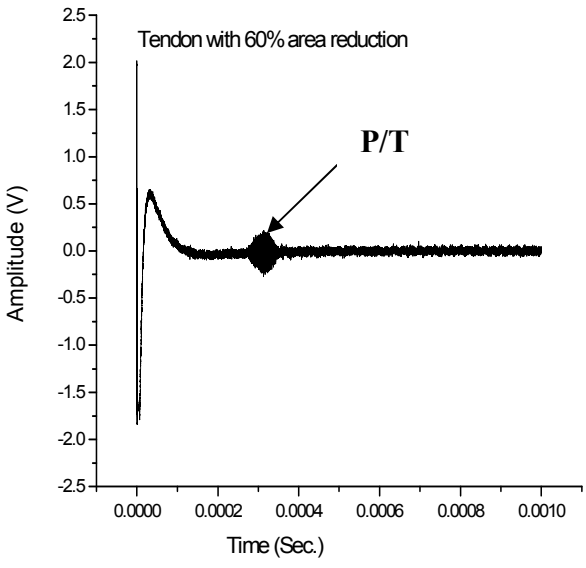

(d) 60%

Fig.3.13 (a-d): Pulse Transmission signatures in strands in concrete (Notch at L/2)

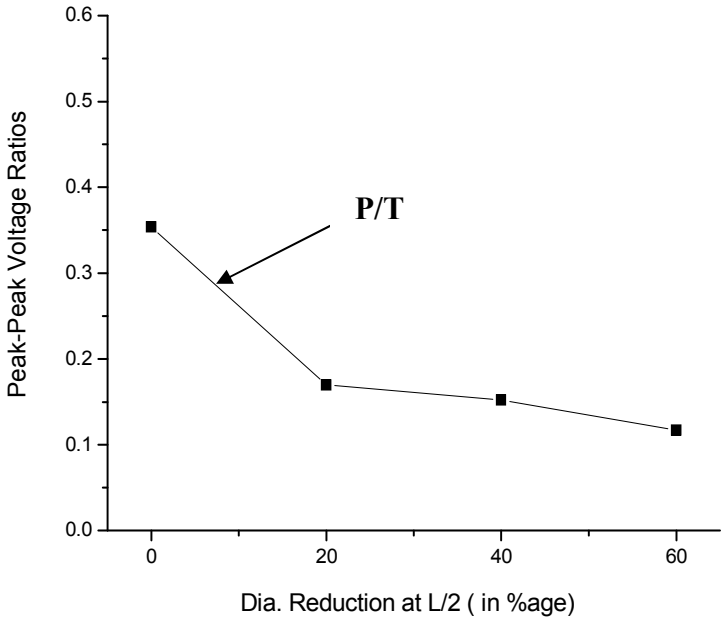

Fig.3.14: Peak to peak voltage ratio trends of P/T in strands in concrete (Notch at L/2)

Effect of variation in damage location of notch

As the damage location was varied from L/2 to L/3 in the strand, the results follow same trends for peak to peak voltage amplitudes in Pulse Transmission testing as for strand with notch at centre **(Fig.3.15)**. Extent of damage can be judged from the peak to peak voltage amplitude ratios of transmitted pulse. As the % of notch increases, P/T strength falls indicating increase in damage. Location of notch cannot be ascertained from pulse transmission. P/E is a better indicator of location of notch.

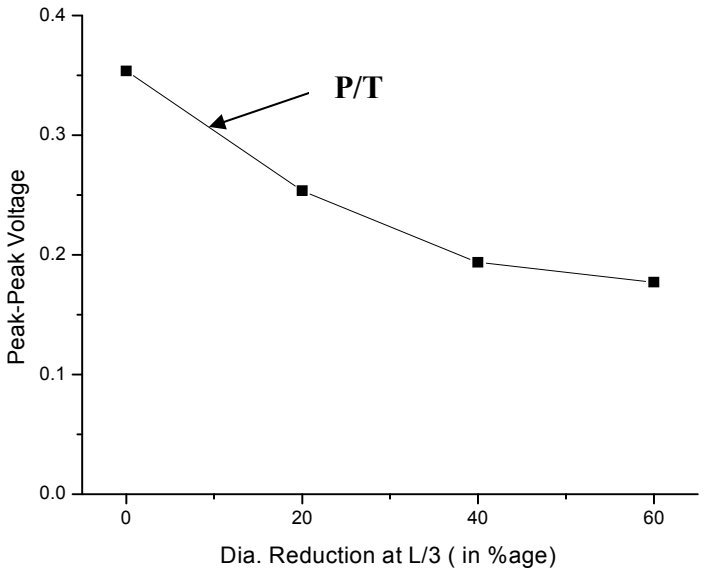

Fig.3.15: Peak to peak voltage ratio trends of P/T in strands in concrete (Notch at L/3)

3.5.2.2 Simulated delamination studies

Damage in the form of delamination or separation is introduced in strand in concrete by winding a double sided tape on the embedded strand in concrete in varying % of extent. % delamination is varied from 0, 25, 50, 75 and 100% along the length of strand and testing is done in P/T mode. The results are plotted in the form of voltage-time curve (V-T). **(Fig.3.16 (a-e))** shows the experimental signatures in P/T studies. **Table 3.4** shows the settings of P/T in strands in concrete with delamination. From these signatures, it can be seen that the percentage of delamination has a strong effect on the V-T curves of **(Fig.3.16 (a-e))**. The extent of damage can be ascertained by observing the peak to peak voltage ratio trend of P/T. As the % of damage increases from 0% to 100%, the magnitude of the transmitted peak increases continuously **(Fig.3.17)** since the amount of leakage into concrete decreases with increases delamination.

Table 3.4 P/T testing in strands in concrete with delamination

JSR DPR 300 Pulser/Receiver settings	
Receiver	
Bandwidth	35
Gain [-12 dB-67 dB]	52 dB
High Pass Filter [Out-12.5 MHz]	Out
Low Pass Filter [3 MHz-35 MHz]	7.5 MHz
Pulser	
Damping [331 ohms-30 ohms]	47 Ohms
Energy [1-4]	4
PRF [100 Hz-5 KHz]	100 Hz
Voltage [100V-400V]	475 V
Impedance [Low-High]	High

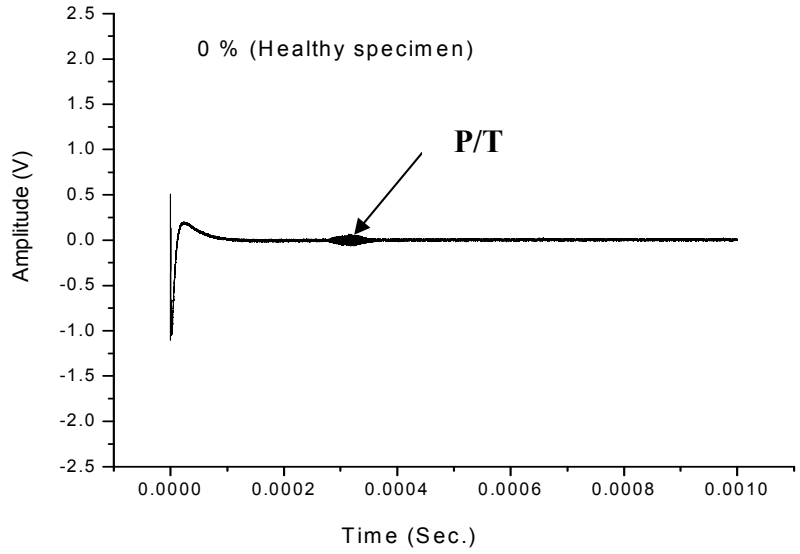

(a) 0%

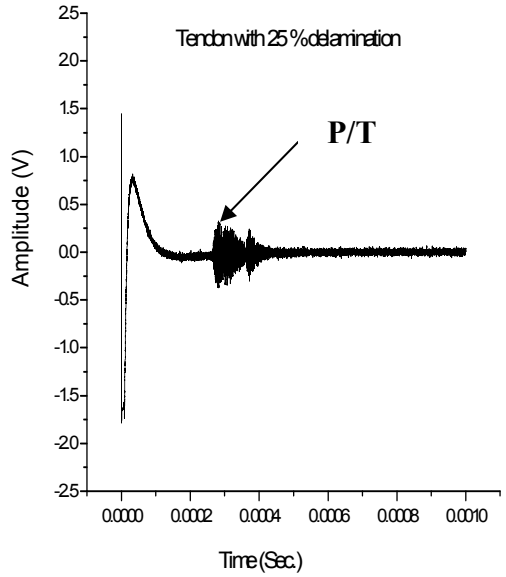

(b) 25%

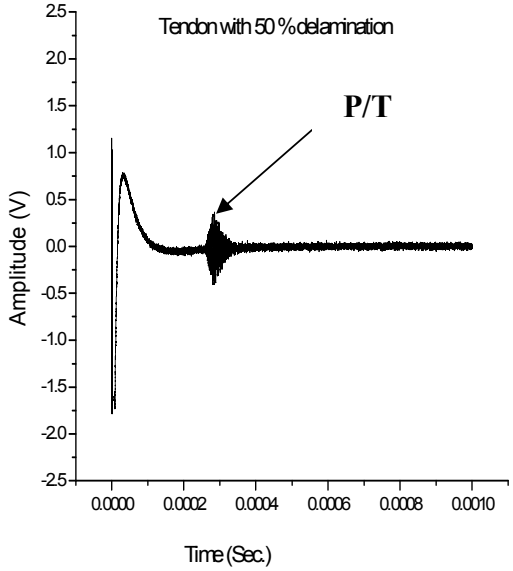

(c) 50%

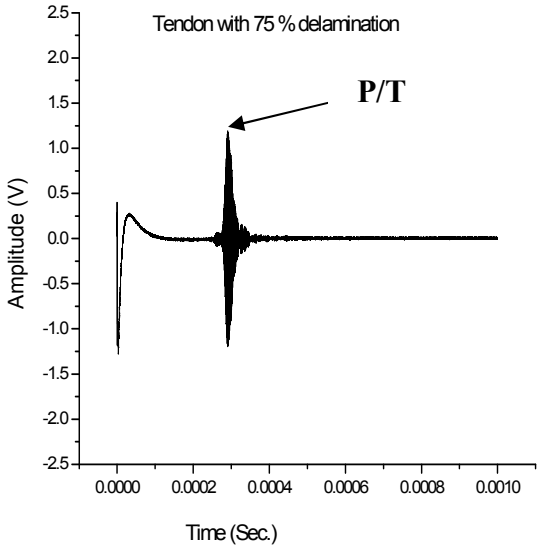

(d) 75%

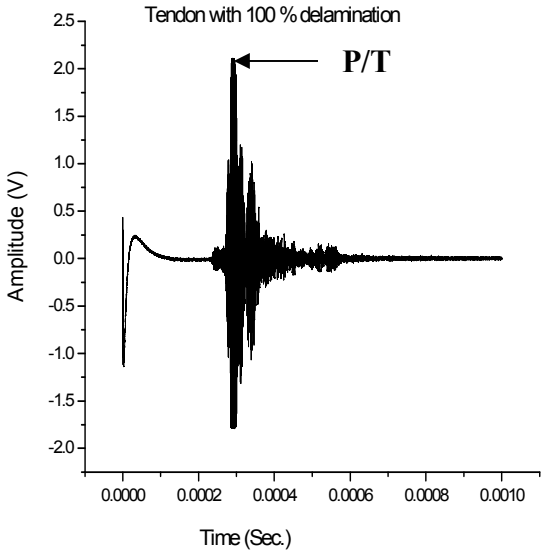

(e) 100%

Fig.3.16 (a-e): Pulse Transmission signatures with 25% , 50%, 75% and 100% delamination in concrete

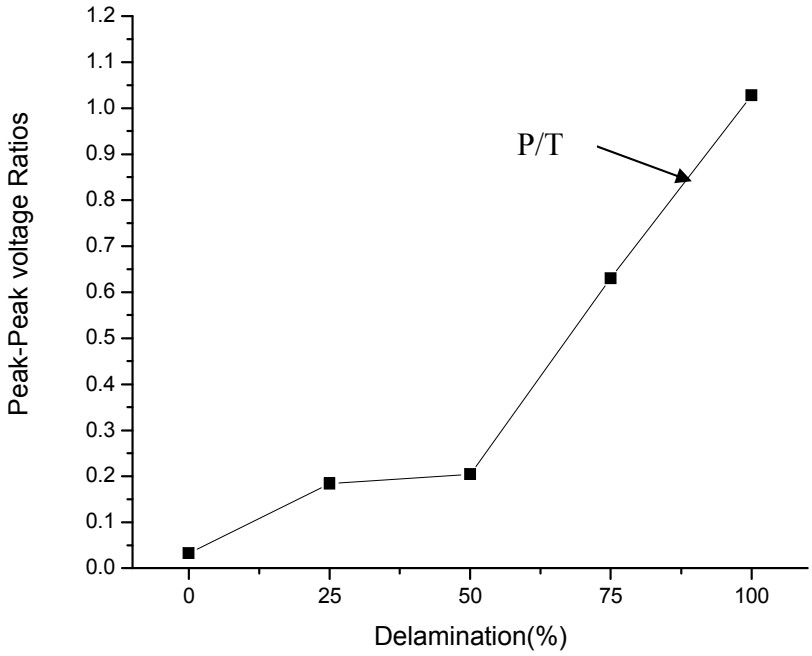

Fig.3.17: Peak to peak voltage ratio trends of P/T with delamination

3.6 CLOSING REMARKS: SIMULATED STUDIES

This study describes an experimental technique for prediction of ultrasonic wave propagation in a strand that has flaws in the form of notches in air as well as when embedded in concrete. The technique not only indicates the presence of damage but also gives the location and magnitude of damage by efficient use of combination of pulse echo and pulse transmission techniques. Location of notch can ascertained from time of flight of NE from pulse echo signatures. Magnitude of notch can judged from P/T in pulse transmission signatures. Both are testing in air as well as in concrete. For simulated delamination studies, P/T increases with increase in % of delamination. Both notching and debonding effects of corrosion had opposing effect on P/T. Hence, it is not possible to pick up both area reduction as well as delamination effects due to actual corrosion by these techniques. The next chapter focuses on the application of these established techniques for actual corrosion studies.

CHAPTER 4

ULTRASONIC INVESTIGATIONS OF TENDONS- ACTUAL CORROSION

4.1 GENERAL

In this chapter, we are focusing on the application of ultrasonic guided waves techniques for actual corrosion studies. The beam undergoing accelerated chloride corrosion is ultrasonically monitoring for days till the ultrasonic signature completely vanished. Also chloride corrosion leads to pitting inside the strand in the form of area loss due to dissolution of the metal. Pulse transmission is monitoring once every day. The effect of actual corrosion monitoring in beams undergoing corrosion is discussed in this chapter.

4.2 EXPERIMENTAL SPECIMEN DETAILS

In natural environments, corrosion takes several years to occur. Hence, the process was accelerated using impressed current. Concrete with proportions of cement, sand and stone aggregates as 1:1.5:3 was taken. The water cement ratio was 0.5. RC beams specimens of dimensions 150 mm x 150 mm x 700 mm were cast. One 12.7 mm diameter pre-stressing steel strand of 1.2 m length was placed at the centre of cross section of the beam at the time of casting. The strand projected out by 250 mm on each side of the beam. The middle 300 mm was selected for exposure to corrosive environment. A thick cotton gauge was placed in this region to keep it moist. Stainless steel wire mesh was wrapped on the cotton gauge. A constant voltage of 30V was applied between the two terminals by means of a constant power supply device. Positive terminal of the power supply was attached to the projected strands in the beam. The negative terminal was connected to the wire mesh. A dripping mechanism was fitted on the wire mesh to keep the cotton underneath saturated. For chloride corrosion 5% Nacl solution was used as drip. Cotton gauge below the wire mesh uniformly distributed the water in the central wrapped portion of the beam **(Fig.4.1)**.

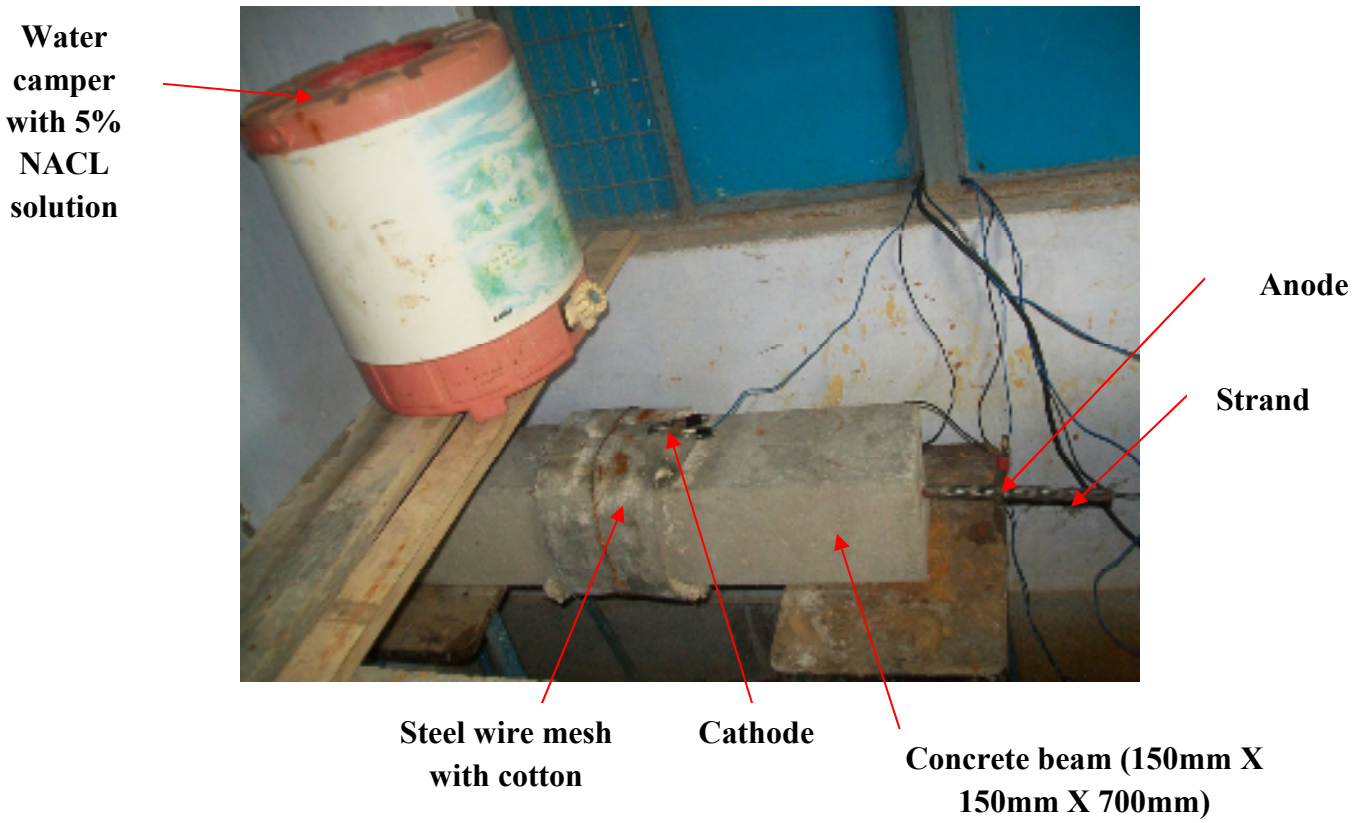

Fig.4.1: Experimental setup

Same ultrasonic set up consisting of pulser/receiver module, transducers and display devices are used for ultrasonic investisation. Same modes and frequency for excitation is used for pulse transmission investigation. During P/T testing external voltage source is switched off.

4.3 RESULTS AND DISCUSSIONS

4.3.1 Visual observations

When a constant voltage of 30 V is applied between two terminals by means of a constant power supply device, beam undergoing accelerated chloride corrosion shows reddish brown patches of corrosion products and, horizontal and vertical cracks appeared on two faces of the beam within 4 days. The cracks divided the entire beam into wedges **(Fig.4.2)**. The cracks initiated at the surface of the beam and progressed along the direction of the reinforcement. Hence, chloride corrosion results in formation of cracks accompained by oozing out of liquid corrosion product

and rust stains. The extruded strand shows significant pits and irregularities on its surface and significant surface changes **(Fig.4.3)**. The loss of metal and crevices is noticed at few places.

Fig.4.2: Beam showing cracks and corrosion product

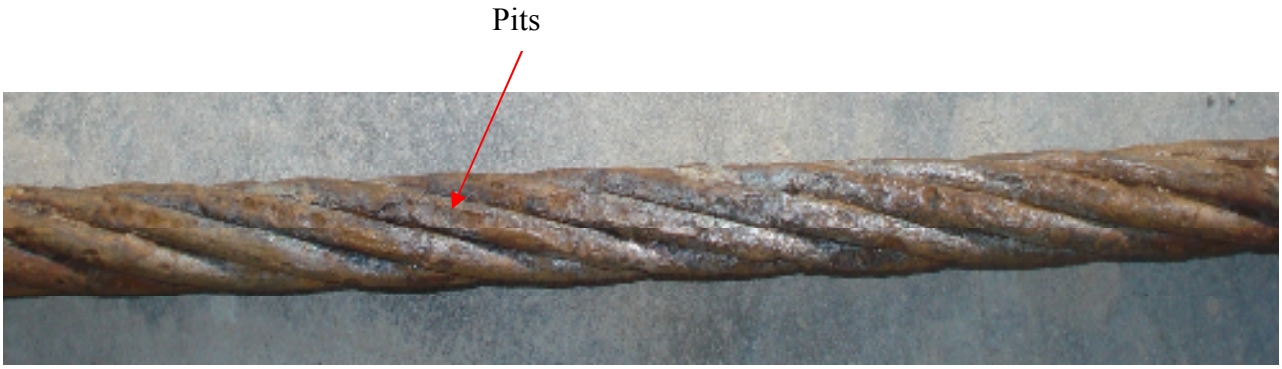

Fig.4.3: Strand showing pits and irregularities on its surface

4.3.2 Ultrasonic monitoring

The pulse transmission testing of strand is measured every day. The transmitted pulse is measured as a time signal. The ratio of the peaks of the applied and transmitted pulses is determined. **(Fig.4.4)** shows ultrasonic voltage trends of the received signal with 1 MHz

transducer. Drop in signal amplitude is observed right from 1st day indicating loss of signal strength as corrosion processed. The loss in signal strength is very fast and the signals vanished completely in 4 days. It indicates severe loss of metal and irregularities due to chloride attack. It results in wave scattering and mode conversion causing drop of signal in 4 days. Hence, chloride corrosion in high tension steel is very fast in comparison to normal steel bar of same diameter where it lasts for 8 days.

.

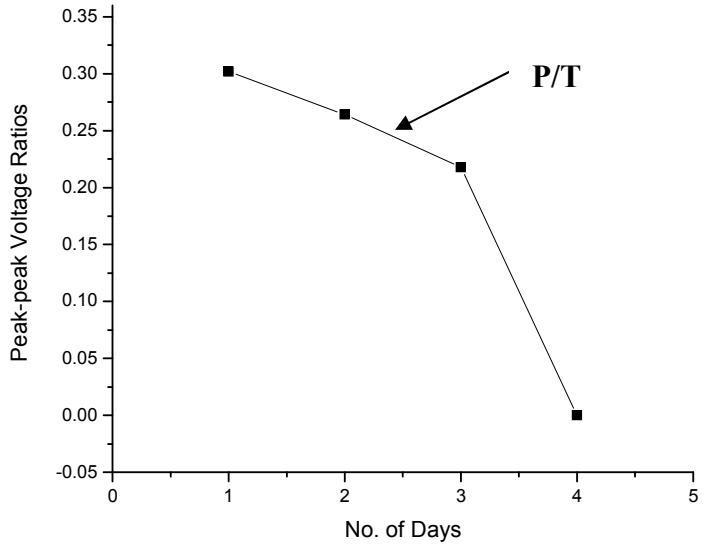

Fig.4.4: Peak-peak voltage ratio trends with L (0, 7) at 1MHz, 12.7 mm diameter (30V)

4.3.3 Effect of variation in voltage

When a constant voltage of 20 V is applied between two terminals by means of a constant power supply device. The results followed same pattern and same trends, but the only difference is on the number of days. It lasts till 10 days. **(Fig.4.5)** shows ultrasonic voltage trends of the received

signal at 1 MHz transducer. Drop in signal is observed right from 1st day and this trend continues till it vanishes in 10 days.

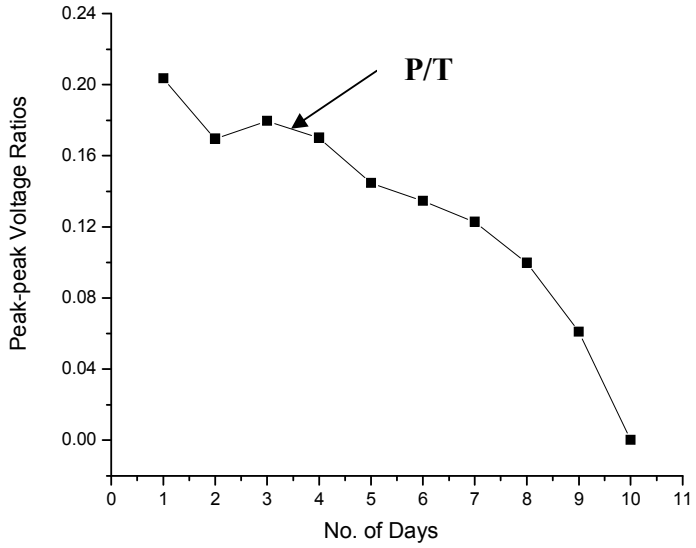

Fig.4.5: Peak-peak voltage ratio trends with L (0, 7) at 1MHz, 12.7 mm diameter (20V)

4.3.4 Effect of variation in diameter of strand

Experiments are also done on 15.8 mm diameter strands. A constant voltage of 30 V was applied between the two terminals by means of a constant power supply device. The results followed same trend. **(Fig.4.6)** shows ultrasonic voltage ratios trend of the received signal at 1MHz transducer.

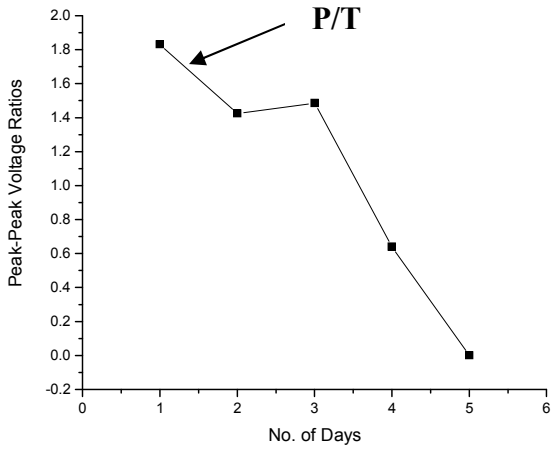

Fig.4.6: Peak-peak voltage ratio trends (30V, 1MHz, 15.8 mm diameter)

4.3.5 Selection of mode to pick up delamination

Monitoring with 1MHz shows severe signal attenuating throughout the corrosion process with L (0, 7) mode. The mode could not pick up delamination phenomenon. The mode shape of the mode was studied **(Fig.4.7 (a & b))** shows that, it is a core seeking mode with all energy concentrated in centre of strand. Hence, it is sensitive to only strand profile changes i.e. pitting.

To pick up surface changes i.e. debonding of the strand, another mode L (0, 1) at 0.1MHz was chosen. It is also a low attenuative mode. **(Fig.4.7 (a & b))** shows that, it is a surface sensitive mode and should pick up debonding. **(Fig.4.8)** shows peak to peak voltage ratio trends of the received signal using surface seeking mode L (0, 1) at 0.1MHz. **(Fig.4.9)** shows the ultrasonic voltage trends of the received signal using core seeking mode L(0, 7) at 1MHz. Thus two different zones are observed in the ultrasonic signal plots:

- First three days had a rising L (0, 1) signal but dropping L (0, 7) signal indicating predominant surface changes. This Zone is referred as '*Delamination Zone*'.

- From third to fifth day, both L (0, 1) and L (0, 7) signals falls and vanishes. At this stage, pitting of the strand is predominant and this zone is referred as '*Pitting Zone*'.

From the ultrasonic plots, the mechanism of corrosion of pre-stressing steel strand in presence of chlorides can be well understood.

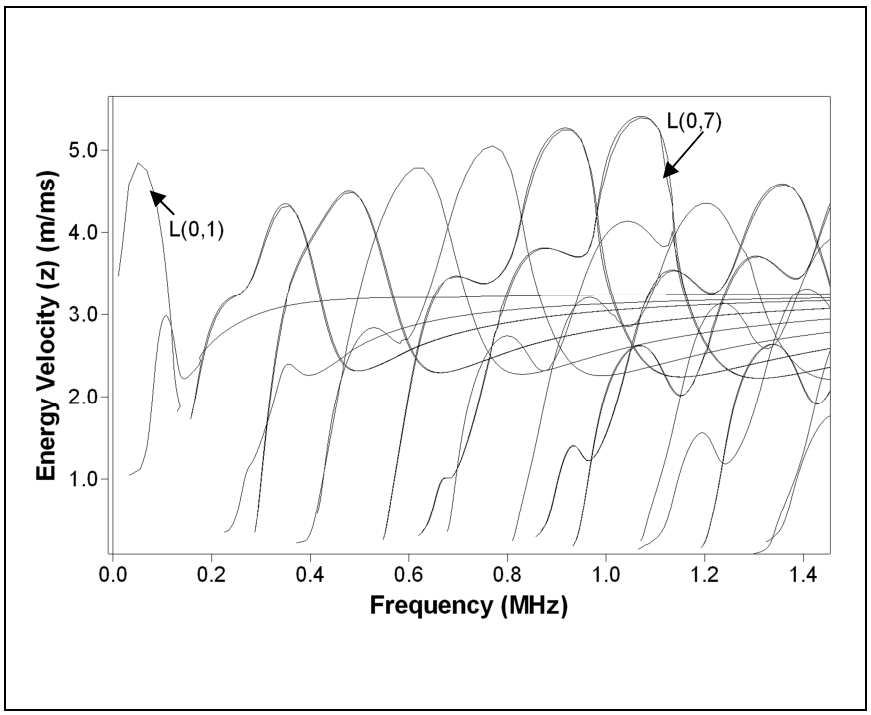

Fig.4.7 (a) Energy Velocity Vs Frequency

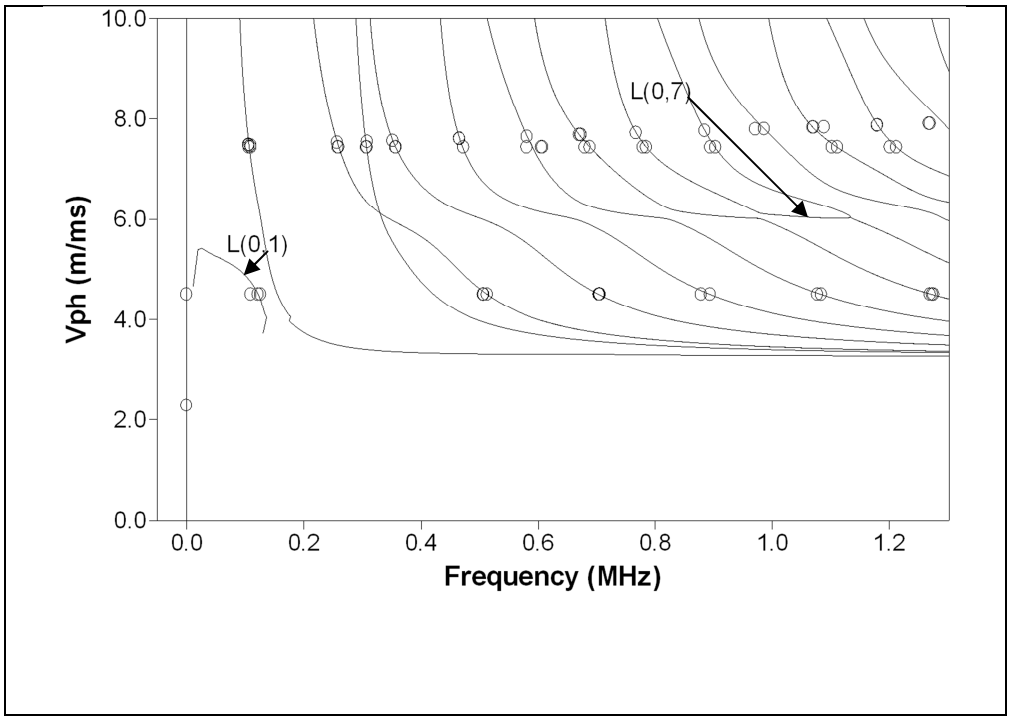

Fig.4.7 (b) Phase velocity Vs Frequency

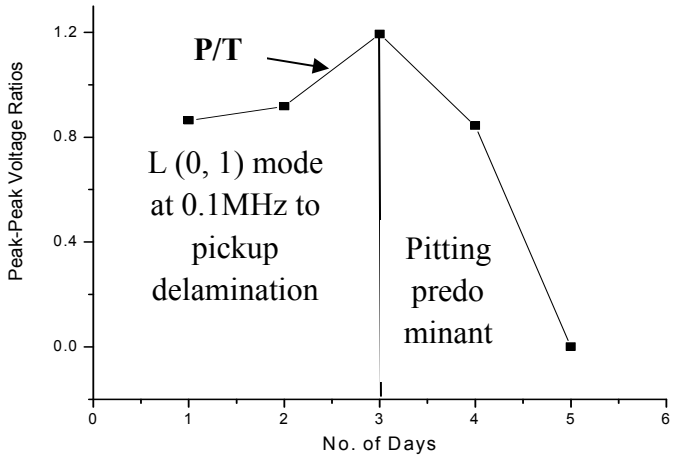

Fig.4.8: Peak-peak voltage ratio trends with L (0, 1) at 0.1MHz, 15.8 mm diameter

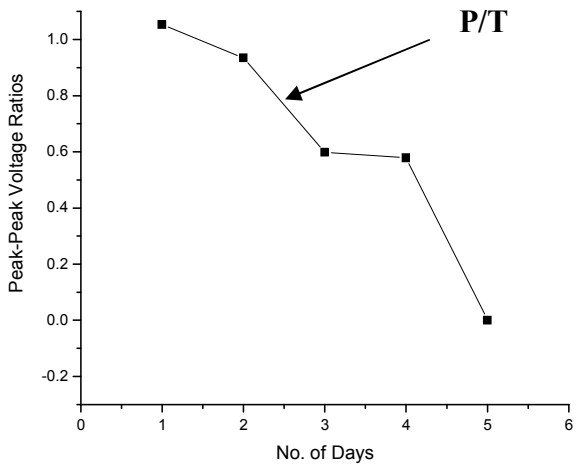

Fig.4.9: Peak-peak voltage ratio trends with L (0, 7) at 1MHz, 15.8 mm diameter

4.4 CLOSING REMARKS: ACTUAL CORROSION STUDIES

In this study, ultrasonic guided waves utilizing core and surface seeking modes can successfully be utilized for monitoring of corrosion in a strand embedded in concrete. In general, corrosion initiates at the surface of the strand leading to the creation of corrosion products that are higher in volume than the surrounding pre-stressing steel. Thus an interfacial bond formation takes place. This is more easily discernible by the L (0, 1) mode that has higher surface component. Hence, to pick up early corrosion L (0, 1) mode is recommended. However, in the presence of chlorides, the strand experiences pitting that lead to deep crevices inside the strand. This is picked up by mode L (0, 7) that has higher component in the core of the strand.

CHAPTER 5

CONCLUSIONS AND FUTURE SCOPE OF WORK

5.1 SUMMARY AND CONCLUSIONS

In this chapter, the conclusions drawn from present work are discussed. Ultrasonic guided waves have been used for inspection of pre-stressing tendons with simulated corrosion damages. P/E and P/T have been used for locality and quantify damages. Then the technique developed is applied to RC with embedded tendons undergoing actual corrosion and the following conclusions have been observed.

5.1.1 Simulated studies

Ultrasonic guided waves are used in experiments for prediction of damages in a strand that has flaws induced in the form of notches and delamination. Testing is first carried out in air and then extended to tendon embedded in concrete. Following conclusions are drawn from the study.

- The technique not only indicates the presence of damage but also gives the location and magnitude of damage by efficient use of combination of pulse echo and pulse transmission techniques.
- Location of notch is ascertained from time of flight of NE from pulse echo signatures.
- Magnitude of notch can be judged from magnitude of transmitted pulse in pulse transmission. It is true for tendons testing in air as well as when embedded in concrete. In concrete, testing is carried out only in pulse transmission mode because of the presence of attenuating concrete, leakage of energy takes place and hence no peaks are obtained in P/E.
- For simulated delamination studies, magnitude of transmitted pulse increases with increase in % of delamination.
- Both notching and debonding effects of corrosion had opposing effect on transmitted peak.

5.1.2 Actual corrosion studies

Ultrasonic guided waves at high frequencies can be effectively used for monitoring simulated damages in pre-stressing strands embedded in concrete by utilizing its wave guide effects. Corrosion has been simulated as loss of bond and loss of area. The results have been compared with that of a strand undergoing accelerated chloride corrosion. Following conclusions are drawn from the study.

- Corrosion in presence of chlorides leads to formation of corrosion products which are voluminous than the surrounding tendon and leads to delamination.
- Further it roughens up the surface of the strand and creates large pittings. Thus, the effect of chloride corrosion is closer to that of a notched tendon.
- Delamination/Debonding is more easily discernible by the low attenuating L (0, 1) mode that has higher surface component. Hence, to pick up early corrosion L (0, 1) mode is recommended.
- However, in the presence of chlorides, the strand experiences pitting that lead to deep crevices inside the strand. This is well picked up by mode L (0, 7) that has higher component in the core of the strand.
- Ultrasonic guided waves utilizing core and surface seeking modes can successfully be utilized for monitoring of corrosion in a strand embedded in concrete.
- It is very essential to select right mode to picking up both delamination and pitting effects of corrosion in tendons.
- In comparison to a reinforcing bar undergoing accelerated corrosion, tendons corrode at a much higher pace. It is due to large surface area of tendons and high tensile strength of steel used.

5.3 FUTURE SCOPE OF WORK

The area of nondestructive testing and damage detection monitoring of tendons in pre-stressed concrete members constitutes the extremely important and challenging area of study where wave propagation provides an efficient means of characterizing defects in structures. As the topic of wave propagation is very wide spread and has utilities in many areas of human endeavor, there is much scope for future work.

The experimentation carried out can be extended for:

- Developing an in-situ damage monitoring technique and set-up utilizing ultrasonic guided waves for damage monitoring in tendons.
- Various issues associated with practical implementation of the same have to be looked into.

REFERENCES

1. Althof, F.C., Inter crystalline Korrosion and Spannungs Korrosion S. 38 ff. Katz. W: Elsen S. 113 ff. In Korrosion und Korrosion-sschitz watter de Gruyter U. Co. Berlin, 1955.
2. Bate S.C.C and E.w. Bennett, Design of Pre-stressed Concrete, Surrey University Press, International Text Book Company Limited, London, 1976, pp 13-16.
3. Bindal, V.N., "Transducers for Ultrasonic Flaw Detection".
4. Beard, M. D., M. J. S. Lowe; and P. Cawley, "Ultrasonic Guided Waves for Inspection of Grouted Tendons and Bolts", 10.1061/ (ASCE) 0899-1561 (2003) 15:3 (212).
5. Bhalla, S., Soh, C. K., Liu, Z., "Wave propagation approach for NDE using surface bonded piezoceramics", NDT & E International 38 (2005) 143-150.
6. Broomfield, J.P., K. Davis, K. Hladky, "The use of permanent corrosion monitoring in new and existing reinforced structure", Cement & concrete composites 24(2002)27-34.
7. Darmawan, M. S., Mark G. Stewart (2006), "Spatial time-dependent reliability analysis of corroding pre-tensioned pre-stressed concrete bridge girders", Structural Safety 29 (2007) 16–31.
8. Dr Sengupta, Amlan K., and Prof. Devdas Menon, "Pre-tensioning systems and devices", section 1.7.
9. F. T. K. Au and J. S. Du, "Prediction of ultimate stress in unbounded pre-stressed tendons", Magazine of concrete Research, 2004, 56, No.1, February, 1-11.
10. Fontana, M. G., Corrosion engineering, Third edition, McGraw-Hill (1986).
11. Francesco Lanza di Scalea; Piervincenzo Rizzo; and Frieder Seible, M.ASCE, "Stress Measurement and Defect Detection in Steel Strands by Guided Stress Waves", 10.1061/(ASCE) 0899-1561 (2003) 15:3(219).
12. Gharighoran, Alireza., Farhad Daneshjoo, Naser Khaji, "Use of Ritz method for damage detection of reinforced and post-tensioned concrete beams", Construction and Building Materials 23 (2009) 2167–2176.
13. www.googleimages.com.

14. Henriksen, C. F., A. Knudsen and M. W. Braestrup, Cable corrosion: Undetected? Concr. Int., 20(10), 50-54 (1998).
15. Jeong-Tae Kim, Jae-Hyung Park , Dong-Soo Hong, Woo-Sun Park, "Hybrid health monitoring of pre-stressed concrete girder bridges by sequential vibration-impedance approaches", Engineering Structures (2009).
16. Joshi, S., Mukherjee, A., and Schmauder S., "Numerical characterization of functionally graded active materials under electrical and thermal fields", Smart Materials and Structures, 12, 571-579 (2003).
17. Kundu, T., T. Gosh, P. Karpur (1998) "Efficient Use of Lamb Modes for Detecting Defects in Large Plates", Ultrasonics 36(2001) 791-801.
18. Kundu, T., Potel, J. F. De Belleval, (2001), "Importance Of Near Lamb Mode Imaging Of Multi Layered Composite Plates", Ultrasonics 39(2001) 283-290.
19. Kundu, T., Young-chul Jung, and Mohammad R. Ehsani, "A New Nondestructive Inspection Technique for Reinforced Concrete Beams", ACI Materials Journal (2002).
20. Kundu, T., Won-Bae Na and M.R. Ehsani, "Lamb waves for detecting delamination between steel bars and concrete", Computer-Aided Civil and Infrastructure Engineering 18 (2003) 58-63.
21. Krishna Raju, N., "Corrosion of high tensile steel in structural concrete", Proceedings of the Journal of Electro-Chemical Society of India, 22(2), 1973, pp 100-105.
22. Li Yibo, Sun Liying, Song Zhidong, Zhang Yuankai (2006), "Study on energy attenuation of ultrasonic guided waves going through girth welds" ScienceDirect Ultrasonics 44 (2006) e1111–e1116.
23. Mukherjee, A., Schmauder, S., Soni, S. S., "Stress Waves in Functionally Graded Materials" M. Tech, dissertation at IIT Bombay (2005).
24. Pievincenzo Rizzo, Elisa sorrivi, Francesco Lanza di Scalea, Erasmo Viola, "wavelet-based outlier analysis for guided wave structural monitoring: Application to multi-wire strands", Journal of sound and vibration 307 (2007) 52-68.
25. Reis, H., Ervin, B.L., Kuchma, D. A., Bernhard, J. T., "Estimation of corrosion damage in steel reinforced mortar using guided waves", Journal of Pressure Vessel Technology, August 2005, Vol. 127/255.

26. Rosenberg, A., C. M. Hansson and C. Andrade, “Mechanisms of corrosion of steel in concrete”, Material science of concrete I, The American Ceramic Society, pp. 258-313 (1989).
27. Schwier, F., “Stress corrosion and relaxation in high-carbon steel wires for pre-stressed concrete”, Wire and Wire Products 1955, pp 1473-1479.
28. Schupack, M., “Durability study of 35 years old post-tensioned bridge”, Concr. Int., 16(2), 50-54 (1994).
29. Schokker, A. J., H. R. Hamilton and M. Schupack, “Estimating post-tensioning grout bleed resistance using a pressure-filter test”, Precast Concr. Inst. J., 47(2), 32-39 (2002).
30. Shivprakash Iyer, Andrea J. Schokker, “Ultrasonic imaging-A novel way to investigate corrosion status in post-tensioned concrete members”, J. Indian Inst. Sci., Sept.-Dec. 2002, 82, 197-217.
31. Shivprakash Iyer and Sunil K. Sinha, “Automated condition assessment of buried sewer pipes based on digital imaging techniques”, J. Indian Inst. Sci., Sep.–Oct. 2005, 85, 235–252.
32. Shruti Sharma, Dr. Abhijit Mukherjee, “Ultrasonics for corrosion monitoring in reinforcing bars in concrete in chloride environment”, ACI (2010).
33. Shruti Sharma, Prashant C. Bhise, Abhijit Mukherjee, “Damage detection in steel bars using ultrasonic guided wave: An Experimental & Analytical Study”, NDT & E-r1-160609 (2010).
34. Vermani Garima under Dr. A. Mukherjee, Ms. Shruti Sharma and Mr. Sandeep Sharma “Damage detection in reinforcing steel bars using ultrasonic wave propagation”, (M.Tech Thesis,Thapar University,Patiala).